Title: Convergent epitope specificities, V gene usage and public clones elicited by primary exposure to SARS-CoV-2 variants

Authors:
Noemia S. Lima[1*], Maryam Mukhamedova[1*], Timothy S. Johnston[1*], Danielle A. Wagner[1*], Amy R. Henry[1], Lingshu Wang[1], Eun Sung Yang[1], Yi Zhang[1], Kevina Birungi[1], Walker P. Black[1], Sijy O'Dell[1], Stephen D. Schmidt[1], Damee Moon[1], Cynthia G. Lorang[1], Bingchun Zhao[1], Man Chen[1], Kristin L. Boswell[1], Jesmine Roberts-Torres[1], Rachel L. Davis[1], Lowrey Peyton[1], Sandeep R. Narpala[1], Sarah O'Connell[1], Jennifer Wang[1], Alexander Schrager[1], Chloe Adrienna Talana[1], Kwanyee Leung[1], Wei Shi[1], Rawan Khashab[2], Asaf Biber[2,3], Tal Zilberman[2,3], Joshua Rhein[4], Sara Vetter[5], Afeefa Ahmed[4], Laura Novik[1], Alicia Widge[1], Ingelise Gordon[1], Mercy Guech[1], I-Ting Teng[1], Emily Phung[1], Tracy J. Ruckwardt[1], Amarendra Pegu[1], John Misasi[1], Nicole A. Doria-Rose[1], Martin Gaudinski[1], Richard A. Koup[1], Peter D. Kwong[1], Adrian B. McDermott[1], Sharon Amit[6], Timothy W. Schacker[4], Itzchak Levy[2,3], John R. Mascola[1], Nancy J. Sullivan[1], Chaim A. Schramm[1#], Daniel C. Douek[1#]

Affiliations:
1. Vaccine Research Center, National Institute of Allergy and Infectious Diseases, National Institutes of Health. Bethesda, MD 20892, USA.
2. Infectious Disease Unit, Sheba Medical Center, Ramat Gan 5262112, Israel.
3. Sackler Medical School, Tel Aviv University, Tel Aviv 6997801, Israel.
4. Department of Medicine, University of Minnesota Medical School, Minneapolis, MN 55455, USA.
5. Minnesota Department of Health, St Paul, MN 55164, USA
6. Clinical Microbiology, Sheba Medical Center, Ramat-Gan 5262112, Israel.
*equal contribution
#correspondence to chaim.schramm@nih.gov and ddouek@nih.gov

Abstract:

While humoral immune responses to infection or vaccination with ancestral SARS-CoV-2 have been well-characterized, responses elicited by infection with variants are less understood. Here we characterized the repertoire, epitope specificity, and cross-reactivity of antibodies elicited by Beta and Gamma variant infection compared to ancestral virus. We developed a high-throughput approach to obtain single-cell immunoglobulin sequences and isolate monoclonal antibodies for functional assessment. Spike-, RBD- and NTD-specific antibodies elicited by Beta- or Gamma-infection exhibited a remarkably similar hierarchy of epitope immunodominance for RBD and convergent V gene usage when compared to ancestral virus infection. Additionally, similar public B cell clones were elicited regardless of infecting variant. These convergent responses may account for the broad cross-reactivity and continued efficacy of vaccines based on a single ancestral variant.

One Sentence Summary: WA1, Beta and Gamma variants of SARS-CoV-2 all elicit antibody responses targeting similar RBD epitopes; public and cross-reactive clones are common.

Main Text:

INTRODUCTION

The sustained spread of SARS-CoV-2 infection has resulted in the emergence of virus variants characterized by the accumulation of multiple sequence mutations. Variants that acquired enhanced transmissibility, pathogenicity or a mechanism of immune escape are considered "variants of concern" (VOC), and include Alpha (PANGO lineage B.1.1.7), Beta (B.1.351), Gamma (P.1), Delta (B.1.617.2), and Omicron (B.1.1.529) (*1*). Their ability to escape immune responses elicited by vaccines based on the first reported sequence from Wuhan (PANGO lineage B.1, here called "WA1"), or by previous infection with a different variant, is a major obstacle to efforts to control the pandemic. A better understanding of the similarities and differences in the immune responses induced by each variant will help guide vaccine design strategies to overcome immune evasion by the virus.

Early in the pandemic, D614G was the first amino acid substitution in the Spike protein to become dominant, and it was shown to confer increased infectivity due to improved Spike stability, albeit with higher sensitivity to antibody neutralization (*2, 3*). Over the course of the pandemic, selective immune pressure is proposed to have led to the accumulation of changes in residues targeted for antibody recognition and neutralization, most importantly in the receptor binding domain (RBD) (*4, 5*). N501Y and other substitutions in RBD increase binding affinity to ACE2 and can compensate for affinity-lowering substitutions that are selected by immune pressure (*6-9*). The combination of K417N/T, E484K/A and N501Y substitutions arose independently in the Beta, Gamma and Omicron variants (*10, 11*), with N501Y also present in the Alpha, Theta, and Mu variants, showing convergent viral evolution along these pathways. Changes in the N-terminal domain (NTD), by contrast, are less often convergent across variants, but may also account for epitope disruption (*12*). Although neutralizing antibodies that recognize NTD are less frequent than those binding to RBD (*13-15*), this domain is a major target for non-neutralizing antibodies that can elicit Fc effector functions (*16, 17*). Therefore, neutralizing capacity and Fc-mediated functionality of antibodies induced by WA1 are significantly reduced against these variants. In addition, CD4 and CD8 T cell responses do not seem to be substantially impacted by variant substitutions (*18-22*).

The epitopes on the ancestral virus targeted by the humoral response have been well characterized (*15, 23-31*) and conservation of these regions among VOCs and across a broad range of sarbecoviruses can be readily assessed. Previous studies of the SARS-CoV-2-specific

antibody repertoire have revealed polarization toward usage of specific V_H genes including IGHV3-53, IGHV3-66, IGHV3-30 and IGHV1-2 (*28, 32-36*). In many cases, convergent V(D)J rearrangements (so-called "public clones") have been found in multiple individuals and several structural classes have been identified (*37*) which comprise antibodies derived from the same genetic elements with a shared binding mode (*13, 27, 30, 33, 38-41*). Many of the most common neutralizing antibodies from these classes make contact with residues such as K417 and E484 and thus lose potency against VOCs (*6, 42*), although some can maintain potency through specific substitutions that adjust the binding conformation to avoid variable residues (*43, 44*). However, neutralizing antibodies make up only a minority of the total binding repertoire, which has not been well characterized in VOC infections compared to WA1.

In-depth characterization of antigen-specific B cell repertoires requires rapid, high-throughput monoclonal antibody (mAb) discovery and functional testing. Further, high-resolution observations of differences in immune responses to SARS-CoV-2 variants can be leveraged to inform future rational vaccine design for boosters and an efficacious pan-coronavirus vaccine. Using a novel method for high-throughput, cloning-free recombinant mAb synthesis and sequencing, we investigated the differences in epitope targeting, V_H gene usage, and B cell clonal repertoires from convalescent individuals infected with WA1, Beta, or Gamma variants.

RESULTS

Spike binding antibody titers in WA1-, Beta-, and Gamma-infected individuals

We collected serum or plasma and PBMC from individuals infected with WA1, Beta, or Gamma variants at 17-38 days after symptom onset (Table S1) to compare antibody and B cell responses. The infecting variant for Beta and Gamma cases was confirmed by sequencing; WA1 cases were from early in the pandemic, prior to the rise of VOCs. All individuals were previously naïve to SARS-CoV-2. As we were interested in studying the total antigen-specific B cell repertoire, we did not select individuals based solely on high neutralization titers, but rather focused on the time post-infection when frequencies of B and T cells are typically high.

We measured serum binding titers to stabilized Spike trimer (S-2P) from WA1, Alpha, Beta, Gamma, and Delta variants, and to RBD from WA1, Alpha, Beta, and Gamma variants using a Meso Scale Discovery electrochemiluminescence immunoassay (MSD-ECLIA) (Fig. 1A). Additionally, we assessed binding titers to Spike from WA1 (with and without D614G), Alpha, Beta, Gamma, Delta, or Omicron variants expressed on the surface of HEK293T cells (Fig. S1A).

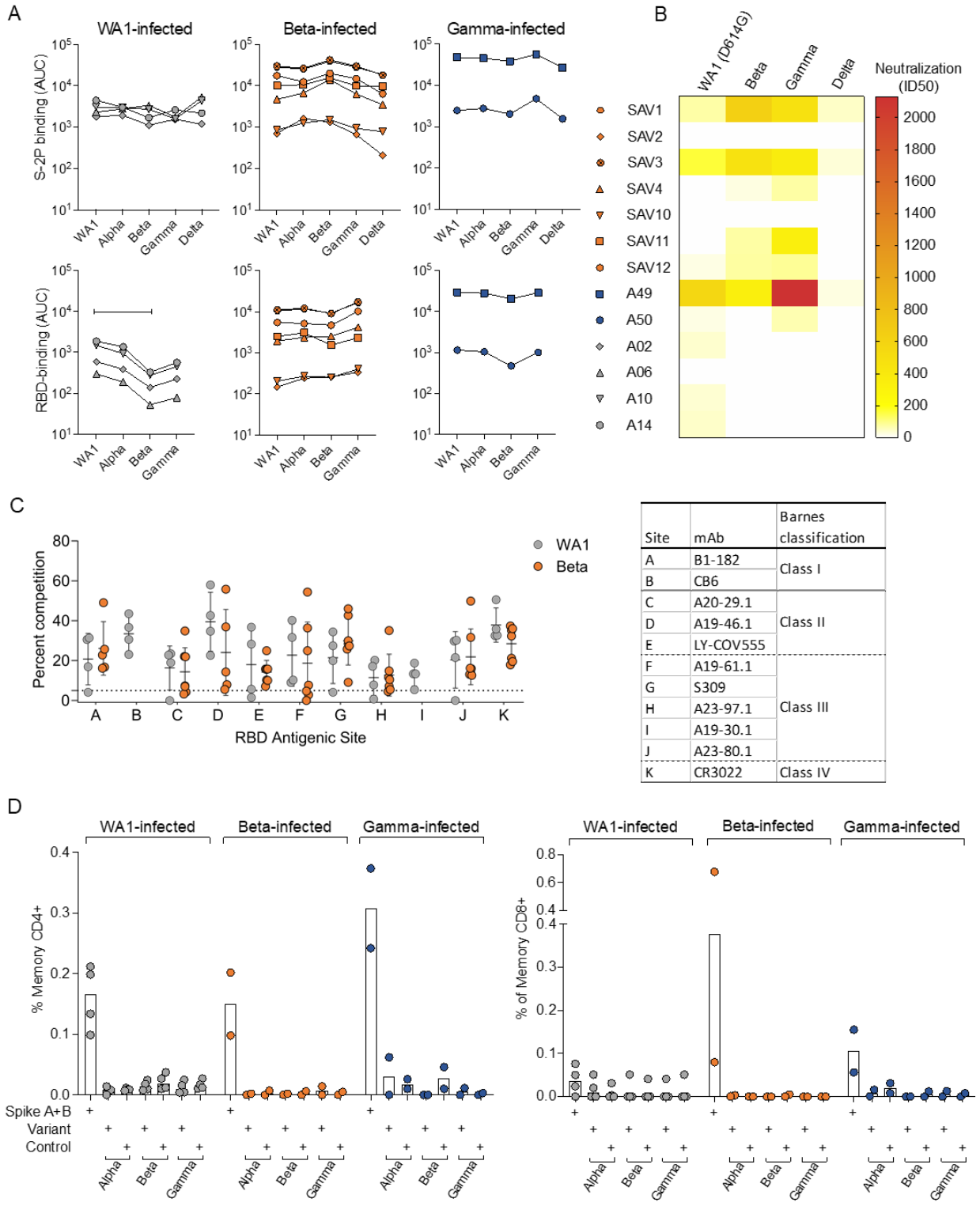

Site	mAb	Barnes classification
A	B1-182	Class I
B	CB6	
C	A20-29.1	Class II
D	A19-46.1	
E	LY-COV555	
F	A19-61.1	Class III
G	S309	
H	A23-97.1	
I	A19-30.1	
J	A23-80.1	
K	CR3022	Class IV

Figure 1: Homologous and cross-reactive antibodies induced by WA1 and variant infections. (**A**) Binding antibody titers to spike (top panels) and RBD (bottom panels) from different variants indicated on the x-axis. (**B**) Heatmap showing neutralizing antibody titers (reciprocal 50% inhibitory dilution) for each individual labeled on the left against each variant indicated on the top. (**C**) Epitope mapping on homologous spike by competition assay using surface plasmon resonance. Antibodies CB6 (RBD-B epitope) and A19-30.1 (RBD-I) do not bind to Beta and competition is not measured at these sites. (**D**) CD4 (left) and CD8 (right) T cell responses to WA1 spike peptide pools A+B, selected pools containing altered variant peptides and control pool containing correspondent peptides for each variant pool.

Both assays showed that all convalescent individuals had antibodies against the homologous Spike as well as cross-reactive antibodies to Spike from other variants. The WA1-infected individuals showed a significant reduction in antibody titers against beta RBD, but variant-infected individuals recognized WA1 RBD at similar levels as the homologous RBD (Fig. 1A), consistent with previous reports (*45, 46*). Individuals with the highest serum binding titers (SAV1, SAV3 and A49) could cross-neutralize WA1, Beta, Gamma, and, with lower potency, Delta variants, however, low levels of neutralization were detected in the other serum samples (Fig. 1B).

VOC infection does not alter B or T cell immunodominance profiles

We next used a surface plasmon resonance (SPR)-based competition assay (*47, 48*) to characterize epitopes targeted by serum antibodies. We individually blocked specific RBD epitopes on S-2P using structurally validated mAbs (Figure S1B) and measured the fraction of polyclonal serum binding activity remaining compared to unblocked trimer. Notably, when the binding activity of each serum was characterized against the homologous Spike, the patterns of reactivity were comparable between individuals infected either with WA1 or Beta (Fig 1C), revealing a similar immunodominance hierarchy across variants. Likewise, there were no differences in competition at each epitope when sera from Beta- or Gamma-infected individuals were mapped against WA1, Beta, or Delta Spike (Fig. S1, C and D). Only one of the WA1-infected individuals produced sufficiently high binding titers against variant Spike to enable epitope mapping by competition (Table S2).

We evaluated the ability of T cells elicited by Beta and Gamma infections to recognize WA1 Spike peptides by measuring upregulation of CD69 and CD154 on CD4 T cells, and production of IFN-γ, TNF, or IL-2 by CD8 T cells (Fig. S1E). Due to PBMC availibility, the Beta-infected individuals included in this analysis were from a different cohort. CD4 and CD8 T cell responses to WA1 Spike peptides were similar in Beta- and Gamma-infected individuals compared to WA1-infected individuals (Fig. 1D). When stimulated with selected peptides covering only regions containing substitutions in each variant, CD4 and CD8 T cell responses were minimal, suggesting that the substituted residues are not included within immunodominant T cell epitopes (Fig. 1D).

High-throughput mAb production and repertoire characterization

The three individuals in our cohort with the highest binding titers (Fig 1A) were selected for in-depth characterization of the antibody repertoire and identification of mAb binding patterns. Two individuals (SAV1 and SAV3) had been infected with the Beta variant, and the third (A49)

156 with Gamma (Fig S2A). To swiftly characterize antibodies from single B cells, we developed a
157 method for rapid assembly, transfection, and production of immunoglobulins (abbreviated to
158 RATP-Ig) that enables high-throughput discovery of mAbs from single-sorted B cells. RATP-Ig
159 relies on 5'-RACE and high-fidelity DNA assembly to produce recombinant heavy and light chain-
160 expressing linear DNA cassettes. These cassettes can be synthesized within two days after
161 single-cell sorting and can be directly transfected into 96-well microtiter mammalian cell cultures.
162 Resulting culture supernatants containing the expressed mAbs can then be tested for functionality
163 (Fig. 2). We sorted cross-reactive $WA1^{+}Beta^{+}$ B cells using S-2P, RBD, or NTD probes (Fig. S2B)
164 from the three selected individuals, resulting in a total of 509 single cells for analysis (Fig. 3A).
165 We recovered paired heavy and light chain sequences from 355 (70%) of cells (Fig. 3A). In
166 parallel, we screened the RATP-Ig supernatants by ELISA for binding to Spike, RBD, and NTD
167 derived from each of WA1, Beta, and Gamma variants. IgG binding at least one antigen was
168 produced in 240 (47%) of wells with a single sorted B cell (Fig. 3, A and B). All three individuals
169 yielded high levels of cross-reactive antibodies to Spike, NTD, and RBD (Fig. 3B and Tables S3-
170 S5). Antibodies isolated from Beta-infected individuals SAV1 and SAV3 showed similar binding
171 profiles dominated by cross-reactive mAbs among WA1, Beta, and Gamma variants (Fig. 3B).
172 While the majority of antibodies isolated from individuals A49 were also cross-reactive, we
173 isolated a large population of Gamma-specific S-2P binding mAbs and another population whose
174 epitope specificity was indeterminate and appeared to bind both RBD and NTD (Fig. 3B and Table
175 S5), perhaps due to high background ELISA signal.

176 We next performed D614G pseudovirus neutralization screening for all supernatants at a
177 4-fold dilution. This assay identified 7, 6, and 1 neutralizing antibodies from individuals SAV1,
178 SAV3, and A49, respectively (Fig. 3C). Neutralizing antibodies were predominately cross-reactive
179 and RBD-specific, except for two which bound to S-2P only and a single NTD-specific antibody
180 (Fig. 3C). RBD-specific neutralizing antibodies were also the most potent of those isolated, with
181 6/12 neutralizing >90% of pseudovirus at 4-fold dilution. It is important to note that supernatant
182 IgG titers were not calculated but were only verified to reach a minimum cutoff value for functional
183 assays, limiting our ability to compare potency between antibodies. Overall, we found that
184 infection with Beta or Gamma variants elicited robust B-cell responses with cross-reactive binding
185 and neutralizing mAbs.

186 To validate our results from supernatants produced by RATP-Ig, we selected seven
187 antibodies for heavy and light chain synthesis and expression. After performing antigen-specific
188 ELISA on the plasmid-transfected supernatants, we found RATP-Ig screening to be reliably
189

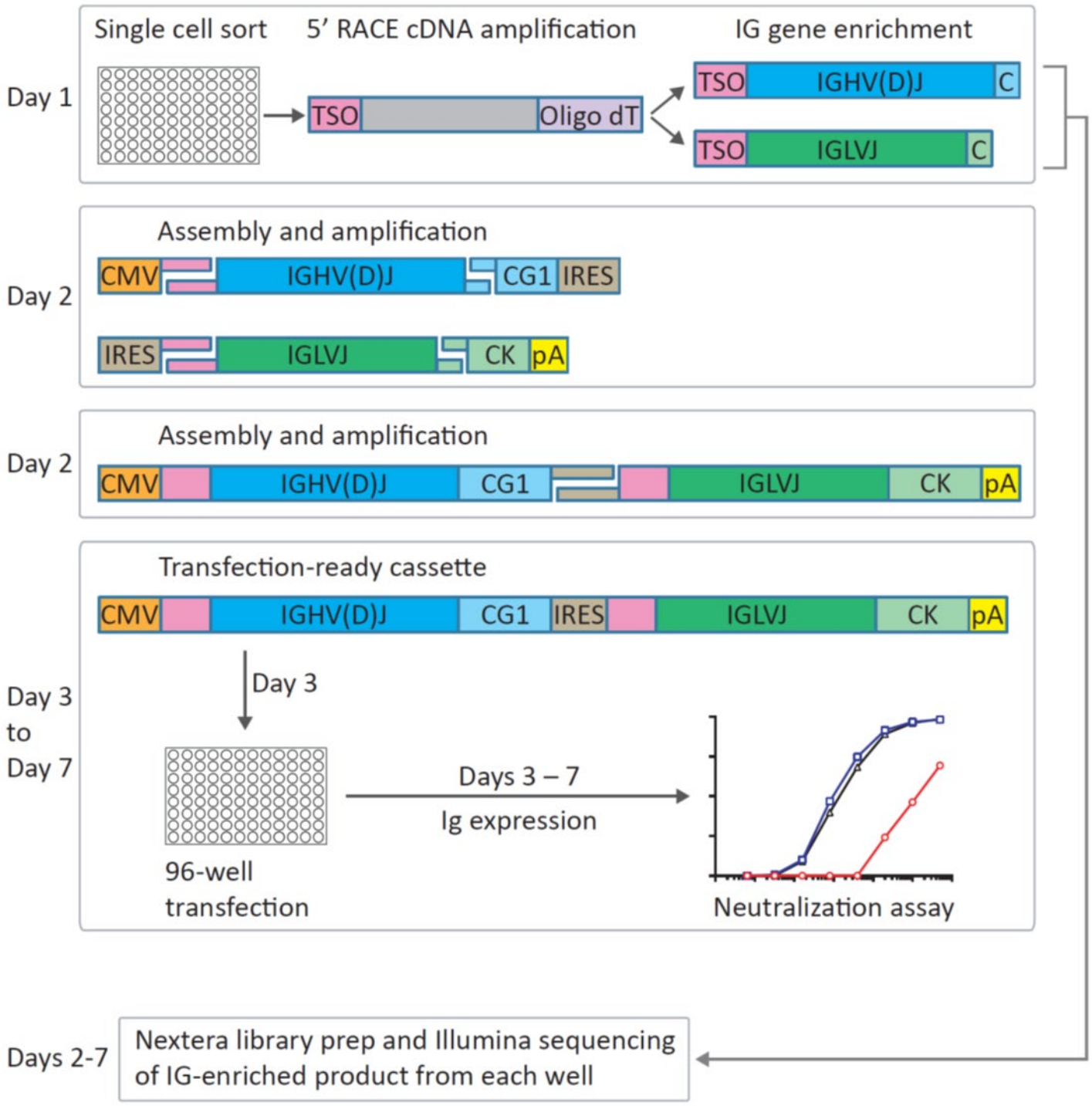

Figure 2: Rapid assembly, transfection and production of immunoglobulin (RATP-Ig) workflow. 5'-RACE is used to generate total cDNA. Full-length heavy and light chain immunoglobulin V genes are enriched by PCR and assembled into recombinant mAb linear expression cassettes. In parallel, V gene libraries are synthesized and sequenced by NGS. Final cassettes are transfected into 96-well Expi293 microtiter cultures, and culture supernatants are collected up to 7 days after initial sort for functional screening.

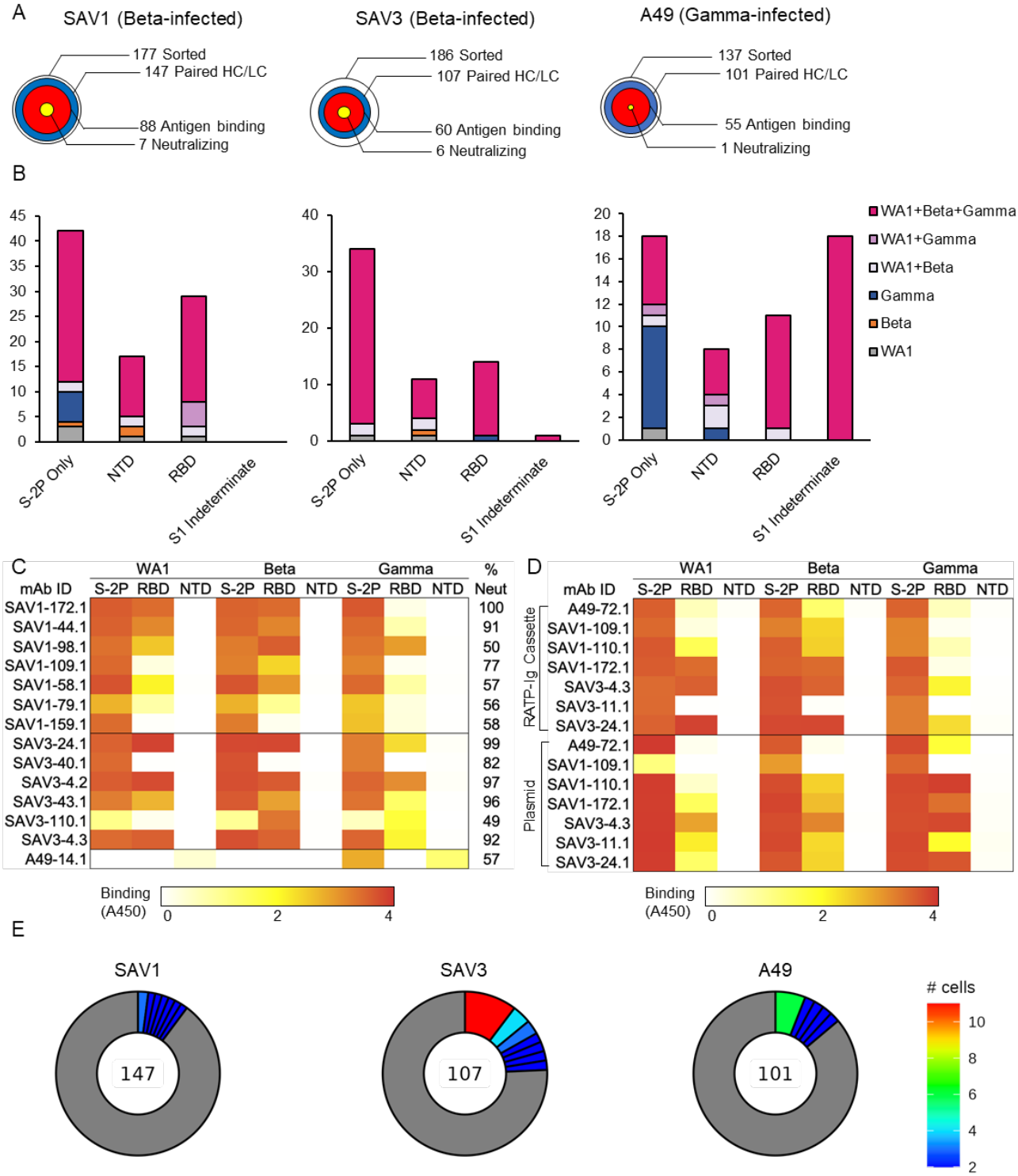

Figure 3: Functional Characterization of RATP-Ig Isolated mAbs. (**A**) RATP-Ig screening overviews for three individuals, represented as bullseyes. The area of each circle is proportional to the number of antibodies. (**B**) Supernatants were screened for antigen-specific binding by single-point ELISA for WA1, Beta, and Gamma S2P, RBD, and NTD. (**C**) Neutralization screening of isolated antibodies at 4-fold supernatant dilutions using a D614G pseudovirus luciferase reporter assay, reported as % virus neutralized derived from reduction in luminescence. Associated ELISA heatmap reported as absorbance at 450nm. (**D**) Validation of RATP-Ig screening with synthesized plasmids. (**E**) Clonal expansion in each individual. Expanded clones are colored by the number of cells in each clone as shown; singleton clones are shown in gray.

204 predictive of mAb functionality, with 59/63 (94%) of functional interactions being reproduced (Fig.
205 3D).

206 While all three individuals had polyclonal antigen-specific repertoires (Fig. 3E), SAV3 and
207 A49 had highly expanded clones matching a widely reported public clone using IGHV1-69 and
208 IGKV3-11 (*28, 34, 49-53*). Members of this public clone were also recovered from SAV1, although
209 they were not greatly expanded. RATP-Ig ELISA data indicated that these antibodies bound a
210 non-RBD, non-NTD epitope on Spike, consistent with available data for previously described
211 members of this public clone. In addition, most antibodies from this public clone have been
212 reported to bind SARS-CoV-1 (*28, 34, 49, 50, 52*), and one, mAb-123 (*50*), weakly binds endemic
213 human coronaviruses HKU1 and 229E.

214 We also found 2 antibodies, SAV1-109.1 and SAV1-168.1, with a YYDRxG motif that can
215 target the epitope of mAb CR3022 on RBD and produce broad and potent neutralization of a
216 variety of sarbecoviruses (*54*). While SAV1-168.1 was cross-reactive but non-neutralizing (Table
217 S3), SAV1-109.1 showed good neutralization potency and bound to all three variants tested when
218 expressed both via RATP-Ig and from a plasmid (Fig. 3, C and D).

219

220 **Sequence analysis of SARS-CoV-2 B cell repertoires elicited by different infecting**
221 **variants**

222 To investigate possible differences in targeting of domains outside of RBD, we stained
223 memory B cells with fluorescently labeled S-2P and individual RBD and NTD probes and
224 examined the specificities by flow cytometry (Fig. S2B). Cells from WA1-infected individuals were
225 stained separately with WA1-, Beta-, and Gamma-based probes, while Beta- and Gamma-
226 infected samples were stained for WA1 and the infecting variant probes (Fig. S2A). As expected,
227 the frequency of antigen-specific cells was generally higher in individuals who had higher serum
228 binding titers, and cells capable of binding to heterologous variants were typically less frequent
229 than those binding the infecting variant (Fig. 4A). In addition, both Beta- and Gamma-infected
230 individuals showed higher frequencies of NTD-binding B cells against the homologous virus when
231 compared to WA1-infected individuals (Fig. 4B).

232 To analyze the SARS-CoV-2 spike-specific B cell repertoire elicited by each variant in
233 more depth, we generated libraries from sorted antigen-specific single cells using the 10x
234 Genomics Chromium platform. After sequencing, we recovered a total of 162, 319, and 107 paired
235 heavy and light chain sequences from WA1-, Beta-, and Gamma-infected groups, respectively
236 (Table S6). As observed in the sequences isolated via RATP-Ig, all three SARS-CoV-2 infected
237

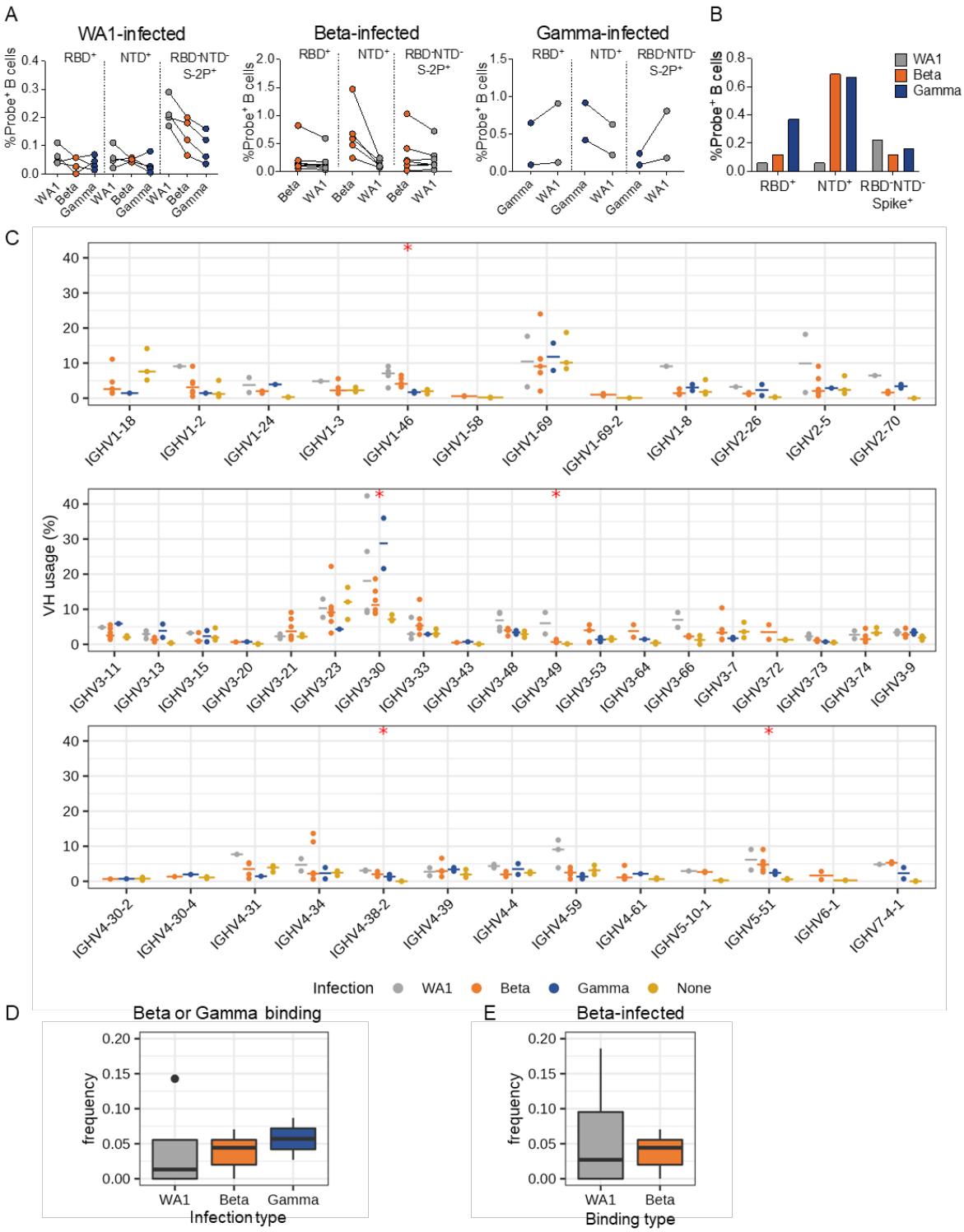

Figure 4: Anti-SARS-CoV-2 Ig repertoires. **(A)** Frequencies of probe+ B cells sorted for IG repertoire analysis. **(B)** Proportion of probe+ B cells binding to each domain. **(C)** SARS-CoV-2-specific VH repertoire analysis by infecting variant WA1, Beta and Gamma shown in grey, orange and blue, respectively, with data from pre-pandemic controls in yellow. X-axis shows all germline genes used; y-axis represents percent of individual gene usage. Stars indicate genes with at least one significant difference between groups; pairwise comparisons are in Table S4. (**D**) and (**E**) Combined frequency of VH genes capable of giving rise to stereotypical Y501-dependent antibodies (IGHV4-30, IGHV4-31, IGHV4-39, and IGHV4-61) in (**D**) Beta- or Gamma-binding B cells from individuals infected with each variant or (**E**) B cells from Beta-infected individuals sorted with either WA1- or Beta-derived probes.

247 IG repertoires showed little clonal expansion. We then combined these data with the sequences
248 generated by RATP-Ig for downstream analysis. Antigen-specific V gene usage was highly similar
249 across all three infection types (Figs. 4C and S3), with differences noted only for IGHV1-46 and
250 IGLV1-47 (Table S7). However, when we compared these specific repertories to the total memory
251 B cell repertoire in pre-pandemic controls (*55*), we observed significant enrichment for several
252 genes (Figs. 4C and S3; Table S7). For example, IGHV1-46, IGHV5-51, and IGLV3-19 were all
253 used at higher levels in both WA1- and Beta-elicited repertoires compared to the total memory
254 pool, while IGHV3-30 was enriched in both WA1- and Gamma-infected individuals compared to
255 controls (adjusted P-value ≤ 0.05, Table S7). This highlights the convergence in responses to all
256 SARS-CoV-2 variants we investigated.

257 Recent studies have shown that Y501-dependent mAbs derived from IGHV4-39 and
258 related genes are overrepresented among neutralizing antibodies isolated from Beta-infected
259 individuals (*56, 57*). Structural evidence suggests that bias toward these genes may in part be
260 due to germline-encoded residues Y35 and Y54 in complementarity-determining region (CDR)
261 H1 and H2, respectively (*56*). We therefore analyzed the observed frequency of germline genes
262 encoding these residues (IGHV4-30, IGHV4-31, IGHV4-39, and IGHV4-61) among Beta- and
263 Gamma-binding B cells but found no significant differences based on infecting variant (Fig. 4D).
264 Furthermore, we compared the frequency of sequences using these germline genes for WA1-
265 versus Beta-binding B cells among Beta-infected individuals (excluding cross-reactive B cells
266 isolated by RATP-Ig), and again found no difference in usage (Fig 4E). In addition, in many of the
267 sequences we observed from these germline genes, Y35 and/or Y54 had been substituted due
268 to somatic hypermutation (SHM), indicating that they likely are not members of the neutralizing
269 class. This suggests that differences in the neutralization sensitivity of variants are not reflected
270 in the overall binding patterns or sequences of specific mAbs, which instead remain highly
271 consistent among individuals infected with different variants.

272 We next investigated SHM levels in these repertoires. The median V_H SHM levels among
273 individuals ranged between 0.3% to 6.6% in V_H and 0.0 to 3.0% in V_L, compared to 6.7% and
274 2.4%, respectively, in the control repertoires. We then further examined SHM by both infecting
275 variant and the probes used to isolate each cell. We found no differences in SHM in single probe-
276 binding repertoires for either WA1- or Gamma-infected individuals (Fig. 5). Surprisingly, cross-
277 reactive (WA1 and Beta) cells sorted for RATP-Ig had lower SHM than the single probe-binding
278 repertoires sorted for 10x Genomics and sequencing. Moreover, single probe-binding Beta-
279 specific B cells from Beta-infected individuals had significantly higher SHM (median of 4.9% in V_H

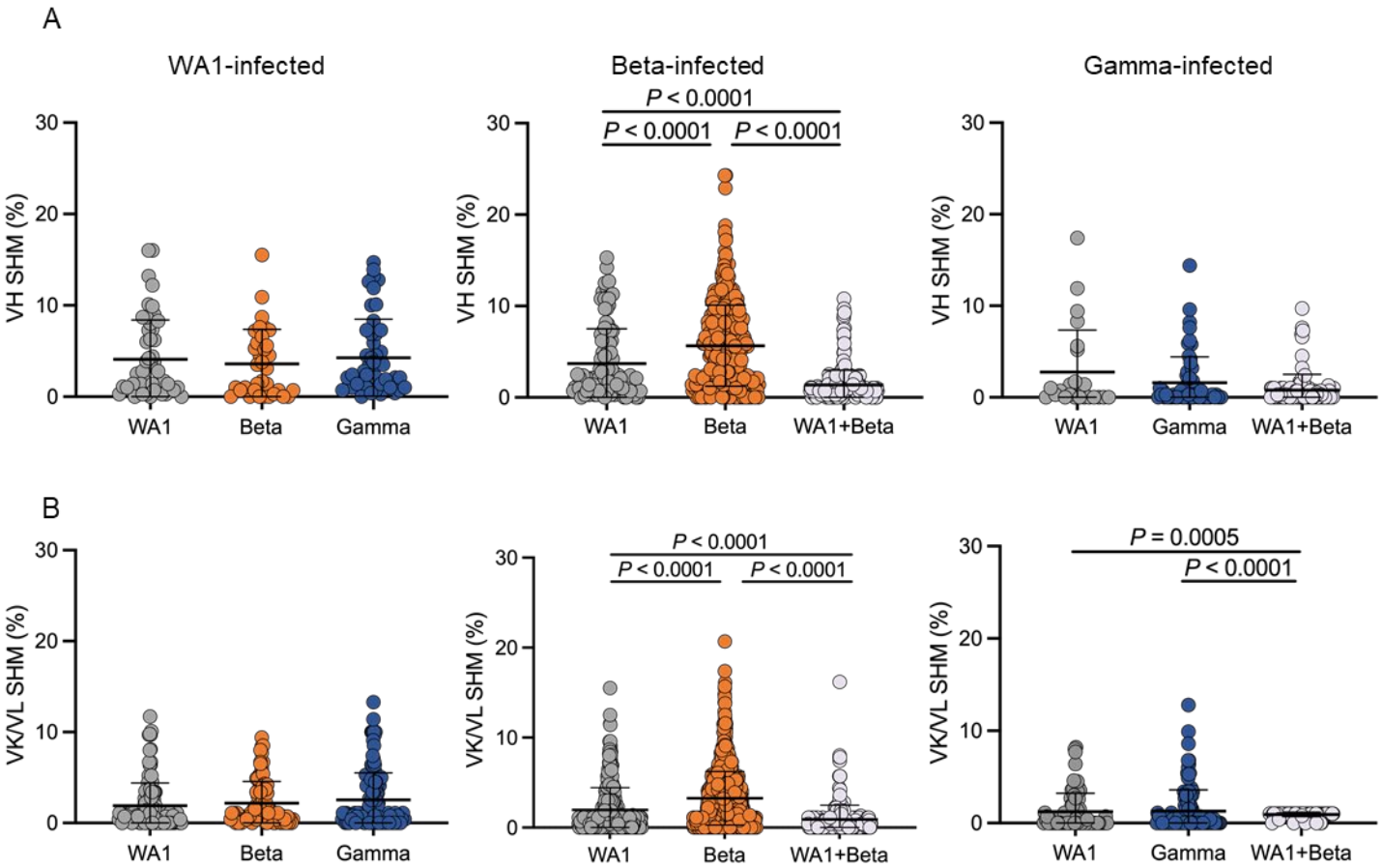

Figure 5: Somatic hypermutation (SHM) levels of SARS-CoV-2 specific B cells (unpaired sequences). SHM percent in variable heavy (V_H) **(A)** or variable kappa/lambda (V_K/V_L) **(B)** regions. Error bars indicate the average number of nucleotide substitutions +/- standard deviation. Statistical significance was determined by the Mann-Whitney t-test.

285 and 2.7% in V_L) compared to single probe WA1-binding cells from the same individuals (2.1% and
286 0.8%, respectively) (Fig. 5). Overall, the low levels of SHM across all the SARS-CoV-2-specific B
287 cells that we isolated is consistent with prior reports (*32, 34, 36, 58-61*). This further demonstrates
288 that the human immune system can readily generate antibodies capable of cross-binding multiple
289 variants, regardless of infecting variant.
290

291 **Identification of public clones**

292 We next identified public clones in the SARS-CoV-2-specific repertoires elicited after
293 infection with different variants. We defined public clones as antibodies from multiple individuals
294 using the same V_H gene and having at least 80% amino acid sequence identity in CDR H3. In
295 total, 16 public clones were identified from 11 of the 13 infected individuals distributed across
296 infection with all three variants (Fig. 6A). Notably, the two people for whom we failed to observe
297 public clones were the least sampled individuals, with only 10 and 16 cells recovered, respectively
298 (Table S6). While light chain V genes and CDR3 were not used to define public clones, they are
299 reported when we found a consistent signature within a public clone.

300 One public clone, found in 5 individuals, uses IGHV4-59 with a short 6 amino acid CDR
301 H3 and IGKV3-20. This public clone comprises B cells from a WA1-infected individual and 4 Beta-
302 infected individuals which bound to both WA1 and Beta probes (Fig. 6A) and has a strongly
303 conserved CDR H3 (Fig. 6B). Antibodies matching the signature of public clone 1 have been
304 previously published (*28, 49, 59, 62-64*); notably, they have been characterized as binding the S2
305 domain of Spike and are generally cross-reactive with SARS-CoV-1. Indeed, one member of this
306 public clone, H712427+K711927, was isolated from an individual who was infected with SARS-
307 CoV-1 (*49*). This suggests that the convergent immune responses we observe may not be limited
308 only to variants of SARS-CoV-2 but may even extend to a broader range of sarbecoviruses.

309 Public clone 2 contains the expanded clones identified by RATP-Ig in SAV3 and A49,
310 discussed above, as well as cells from SAV12. Public clone 3 includes sequences from two
311 individuals that bound to either Beta or Gamma probes. Notably, both public clones 2 and 3 use
312 the same heavy and light chain germline genes with the same CDR H3 and L3 lengths, though
313 they fall outside of the 80% amino acid identity threshold. Combining sequences from both public
314 clones revealed a strongly conserved IGHD3-22-encoded YDSSGY motif at positions 6-11 of
315 CDR H3 (Fig. 6C). Strikingly, this is the same D gene implicated in targeting a Class IV RBD
316 epitope (*54*), although public clones 2 and 3 instead target an epitope in S2 and appear to be
317 restricted to IGHV1-69 and IGKV3-11 V genes.

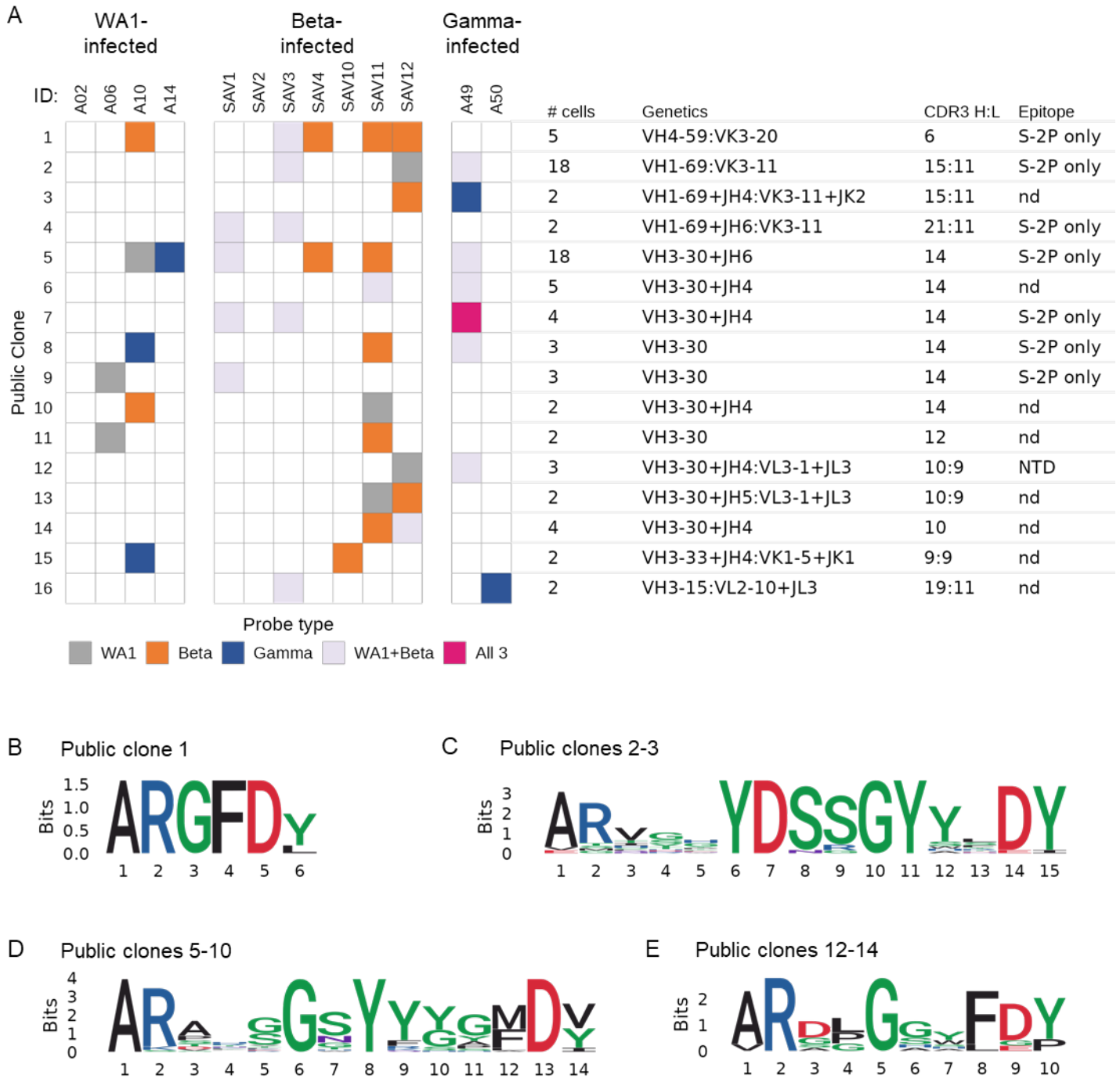

Figure 6: Public and cross-reactive clones. **(A)** Sixteen public clones were identified. Public clones are numbered 1-16 by row, as shown on the far left. Each column of boxes in the middle panel represents a single individual, as labeled at top, and is colored by probe(s) used, as shown at bottom. Right panel shows additional information about each public clone. Light chain ifnormation is provided after a colon if a consistent signature was found. Epitopes are inferred from ELISA of RATP-Ig supernatants of at least 1 public clone member; nd, not determined. **(B)** CDR H3 logogram for the top public clone, found in 5 of 13 individuals. (**C**)-(**E**) Combined CDR H3 logograms for **(C)** 2 public clones using IGHV1-69 and IGKV3-11 with a 15 amino acid CDR H3 length. **(D)** 6 public clones using IGHV3-30 with a 14 amino acid CDR H3 length. **(E)** 3 public clones using IGHV3-30 with a 10 amino acid CDR H3 length.

We also observed the repeated use of IGHV3-30 with a 14 amino acid CDR H3 in six public clones which together comprise 35 cells from 8 different individuals. Each of these public clones included cells that bound to at least two variants, and all six were identified in individuals from at least two of our three variant-infected cohorts, suggesting a common, cross-reactive binding mode. When we combined CDR H3 sequences from all 6 public clones in this group, we found a consistent small-G-polar-Y-aromatic motif spanning positions 5-9 of CDR H3 (Fig. 6D). A large number of antibodies matching this signature have been previously described (*25, 28, 34, 49-52, 59, 60, 62-66*). Similar to the above public clones, the epitope targeted by these antibodies has generally been reported as being in the S2 domain of Spike, and approximately one third of them have been shown to also bind SARS-CoV-1.

We identified only one public clone, 12, that we were able to verify bound to either RBD or NTD, although public clones 13 and 14 also have highly similar V genes and CDR lengths (Fig. 6, A and E). These public clones were identified in both Beta- and Gamma-infected individuals from cells isolated with WA1 and/or Beta probes. Two previously reported antibodies, WRAIR-2038 (*16*) and COV-2307 (*34*), match the signature of these public clones and are also confirmed to bind NTD. The identification of a cross-reactive public clone is remarkable given deletions in Beta that disrupt the main NTD supersite for neutralizing antibodies (*12*). This again highlights the discordance between neutralization, which is variant-restricted, and reproducible binding modes which show a consensus in the face of differences among variants.

DISCUSSION

The rise of novel, antigenically distinct SARS-CoV-2 variants both threatens the efficacy of lifesaving mAb therapies and emphasizes the need for continued therapeutic mAb discovery (*67*). Moreover, although T cell responses are predominantly directed toward conserved epitopes and hence are broadly cross-reactive (*18-22*), Spike-binding IgG antibodies and serum neutralization have been identified as key correlates of protection for SARS-CoV-2 infection (*68-70*). Thus, a deep understanding of the IG repertoires that generate these protective responses will be critical for predicting the impact of infections with different variants.

In this study, we used rapid mAb production and functional analysis and single cell sequencing using the 10x Genomics platform to conduct an in-depth, unbiased characterization of total antigen-specific B cell repertoires from people infected with the ancestral WA1, Beta, or Gamma variants of SARS-CoV-2. Our principal findings were: 1) infection with any of these variants elicited antibodies targeting the same immunodominant epitopes in RBD; 2) antigen-specific memory B cells elicited by SARS-CoV-2 are polyclonal and use similar patterns of heavy

361 and light chain V genes, irrespective of the infecting variant; and 3) public clones and other cross-
362 reactive antibodies are common among responses to all infecting variants. Our results
363 demonstrate a fundamentally convergent humoral immune response across different SARS-CoV-
364 2 variants.

365 To date, most analyses of SARS-CoV-2-specific B cells have focused on neutralizing
366 antibodies with potential therapeutic applications. Those which have investigated the total binding
367 repertoire have used samples from people infected with the ancestral WA1 variant (*9, 25, 31*);
368 here we complement these studies with new data from Beta- and Gamma-infected individuals
369 and show that the hierarchy of immunodominant epitopes remains unchanged. Indeed, while a
370 recent report found that serum antibodies elicited by Beta infection were less likely to contact
371 Spike residue F456 compared to antibodies elicited by WA1 infection (*71*), we found no changes
372 in targeting of the RBD-A epitope, which includes this residue. Combined with the fact that Spike
373 F456 is unchanged between WA1 and Beta, this suggests that the difference in escape is likely
374 due to a shifted binding conformation (*43, 44*). Thus, just as binding epitope immunodominance
375 is known to be consistent in response to WA1, Beta, or Omicron mRNA immunization (*47, 48*),
376 we now demonstrate here similar immunodominance after variant infection. This insight will be
377 helpful for understanding and predicting the burdens of serial infections with different variants.

378 In addition to concordant epitope targeting, we also found consistent V gene usage in the
379 antibody response to all three variants we investigated. Although some recent studies have noted
380 enrichment for IGHV4-39 and closely related V_H genes in Beta-infection (*56, 57*) we did not
381 observe any differences in the usage of these genes. Our findings likely highlight the difference
382 between the neutralizing antibody repertoires investigated in prior studies compared to the total
383 binding repertoires examined here and emphasize the insights to be gleaned by taking a broader
384 perspective. However, despite this consistent epitope immunodominance and convergent V gene
385 usage, we observed an excess of SHM in homologous Beta-binding B cells isolated from Beta-
386 infected individuals, an effect we did not observe in WA1- or Gamma-infected individuals. This is
387 even more unexpected in light of the lower overall SHM in cross-binding B cells sorted for mAb
388 isolation by RATP-Ig. Other studies have also suggested the possibility that Beta may be
389 somewhat distinct from other SARS-CoV-2 variants, inducing neutralization that appears to wane
390 more slowly and that can be boosted to higher levels by additional vaccine doses (*47, 48*). In this
391 light, it is perhaps even more important that we identified the same cross-reactive public clones
392 induced by Beta infection as by WA1 and Gamma, suggesting that key elements for protection
393 against other variants are likely to be maintained.

394 Furthermore, the genetic convergence among IG repertoires was not limited to V gene
395 usage but extended to the public clones we identified. These were reliably observed irrespective
396 of the infecting variant and were consistently identified as cross-reactive to multiple variants.
397 Additionally, members of public clones 1 and 2 have been reported in the literature as having
398 cross-reactivity extending to SARS-CoV-1. While they appear to be non-neutralizing and S2
399 domain-binding, they may yet be important for Fc-dependent functions (*16, 17*) and thus their
400 elicitation by different variants may contribute to protection from future infection with other
401 variants. Overall, more than 8% of the cells that we sequenced belong to a public clone,
402 highlighting again the extraordinary convergence of the antibody response across variants of
403 SARS-CoV-2.

404 Importantly, we also observed convergences that are not encompassed within the
405 standard definition of a public clone, consistent with structural modeling and clustering
406 demonstrating that high CDR H3 sequence similarity and even convergent V genes are not
407 required for antibodies to target overlapping epitopes using comparable binding conformations
408 (*72*). As a specific example, we identified antibodies with a previously described IGHD3-22-
409 encoded YYDRxG motif that can result in broad neutralization of divergent sarbecoviruses (*54*).
410 Furthermore, we also observed three sets of multiple public clones with overlapping gene usage
411 and CDR H3 lengths. Despite the low CDR H3 sequence homology between public clones, we
412 found conserved motifs which are likely to drive functional convergence. These findings further
413 highlight the capability of the human immune system to respond to SARS-CoV-2 in a manner that
414 is largely consistent yet tolerant of differences between variants.

415 In summary, our data reveal marked convergence that defines multiple aspects of the
416 humoral immune response to different SARS-CoV-2 variants. Despite the emergence of key
417 escape mutations which have pronounced impact on neutralizing antibody function, first-
418 generation vaccine designs using the ancestral Spike protein sequence have demonstrated the
419 capacity to generate a cross-reactive anamnestic response that can be mobilized upon infection
420 with novel variants (*47, 48, 73, 74*). Our observations show that this phenomenon may be
421 explained in part by convergent V-gene usage and epitope specificities elicited by primary
422 exposure to SARS-CoV-2 variant Spikes.

423

424 **LIMITATIONS OF THE STUDY**

425 Our study is limited by sampling of paired heavy and light chain sequences from fewer
426 than 1,000 SARS-CoV-2-specific B cells across 13 individuals. This scale is small in comparison
427 to bulk IG sequencing studies (*32, 61*) and even a few single-cell studies (*58, 60, 75*). We are

428 also limited in our ability to make functional repertoire comparisons due to varied sorting strategies
429 and differences in functional assays used to assess isolated mAbs. Moreover, our cohort was
430 sampled only at a single time point early in convalescence and included only one individual with
431 high serum neutralization titers. It will be important to verify that our findings extend to later time
432 points when the antibody repertoire has matured. In addition, further studies are needed to
433 examine the response elicited by more recent SARS-CoV-2 variants such as Delta and Omicron.
434

435 **MATERIALS AND METHODS**

436 **Study design**

437 We selected 13 convalescent individuals that had experienced symptomatic Covid-19
438 infection with either WA1 virus or the Beta or Gamma variants. Serum, plasma and PBMC were
439 isolated at each respective clinical center. The selection of individuals was based on the
440 availability of samples collected at similar time-points (between 17 and 38 days after symptoms
441 onset), rather than the severity of disease or neutralizing antibody titers (Table S1). Seven
442 individuals were infected with the Beta variant and recruited at the Sheba Medical Center, Tel
443 HaShomer, Israel. Two individuals were infected with the Gamma variant and recruited at the
444 University of Minnesota Hospital, USA. The samples from four WA1-infected individuals, collected
445 early in the pandemic, as well as the two additional beta-infected individuals used for T cell
446 analysis were collected under the Vaccine Research Center's (VRC), National Institute of Allergy
447 and Infectious Diseases (NIAID), National Institutes of Health protocol VRC 200 (NCT00067054)
448 in compliance with the NIH Institutional Review Board (IRB) approved protocol and procedures.
449 All subjects met protocol eligibility criteria and agreed to participate in the study by signing the
450 NIH IRB approved informed consent. Research studies with these samples were conducted by
451 protecting the rights and privacy of the study participants. All participants provided informed
452 consent in accordance with protocols approved by the respective institutional review boards and
453 the Helsinki Declaration.
454

455 **Serology**

456 Antibody binding was measured by 10-plex Meso Scale Discovery
457 Electrochemiluminescence immunoassay (MSD-ECLIA) as previously described (*76*). Cell-
458 surface spike binding was assessed as previously described (*76*). Serum neutralization titers for
459 either WA1-D614G, Beta, Gamma or Delta pseudotyped virus particles were obtained as
460 previously described (*76*).
461

462 **Antigen-specific ELISA**

463 Reacti-Bind 96-well polystyrene plates (Pierce) were coated with 100 µl of affinity purified
464 goat anti-human IgG Fc (Rockland) at 1:20,000 in PBS, or 2 µg/ml SARS-CoV-2 recombinant
465 protein in PBS overnight at 4°C. Plates were washed in PBS-T (500ml 10XPBS + 0.05% Tween-
466 20 + 4.5L H2O) and blocked for 1 h at 37ºC with 200 µL/well of B3T buffer: 8.8 g/liter NaCl, 7.87
467 g/liter Tris-HCl, 334.7 mg/liter EDTA, 20 g BSA Fraction V, 33.3 ml/liter fetal calf serum, 666
468 ml/liter Tween-20, and 0.02% Thimerosal, pH 7.4). Diluted antibody samples were applied and
469 incubated 1 hr at 37ºC followed by 6 washes with PBS-T; plates were the incubated with HRP-
470 conjugated anti-human IgG (Jackson ImmunoResearch) diluted 1:10,000 in B3T buffer for 1 h at
471 37ºC. After 6 washes with PBS-T, SureBlue TMB Substrate (KPL) was added, incubated for 10
472 min, and the reaction was stopped with 1N H2SO4 before measuring optical densities at 450nm
473 (Molecular Devices, SpectraMax using SoftMax Pro 5 software). For single-point assays,
474 supernatants from transfected cells were diluted 1:10 in B3T and added to the blocked plates.
475 Purified monoclonal antibodies were assessed using 5-fold serial dilutions starting at 10ug/ml. To
476 assess the levels of IgG in supernatants, standard curves were run on the same plates as
477 supernatants, using threefold serial dilutions of human IgG (Sigma) starting at 100ng/ml IgG.
478

479 **Intracellular cytokine staining**

480 The T cell staining panel used in this study was modified from a panel developed by the
481 laboratory of Dr. Steven De Rosa (Fred Hutchinson Cancer Research Center). Directly
482 conjugated antibodies purchased from BD Biosciences include CD19 PE-Cy5 (Clone HIB19; cat.
483 302210), CD14 BB660 (Clone M0P9; cat. 624925), CD3 BUV395 (Clone UCHT1; cat. 563546),
484 CD4 BV480 (Clone SK3; cat. 566104), CD8a BUV805 (Clone SK1; cat. 612889), CD45RA
485 BUV496 (Clone H100; cat. 750258), CD154 PE (Clone TRAP1; cat. 555700), IFNg V450 (Clone
486 B27; cat. 560371 and IL-2 BB700 (Clone MQ1-17H12; cat. 566404). Antibodies from Biolegend
487 include CD16 BV570 (Clone 3G8; cat. 302036), CD56 BV750 (Clone 5.1H11; cat. 362556), CCR7
488 BV605 (Clone G043H7; cat. 353244) and CD69 APC-Fire750 (Clone FN50; cat. 310946). TNF
489 FITC (Clone Mab11; cat. 11-7349-82) and the LIVE/DEAD Fixable Blue Dead Cell Stain (cat.
490 L34962) were purchased from Invitrogen.

491 Cryopreserved PBMC were thawed into pre-warmed R10 media (RPMI 1640, 10% FBS,
492 2 mM L-glutamine, 100 U/ml penicillin, and 100 µg/ml streptomycin) containing DNase and rested
493 for 1 hour at 37ºC/5% CO_2. For stimulation, 1 – 1.5 million cells were plated into 96-well V-bottom
494 plates in 200mL R10 and stimulated with SARS-CoV-2 peptide pools (2ug/mL for each peptide)
495 for 6 hours at 37ºC/5%CO_2. A DMSO-only condition was used to determine background

496 responses. Following stimulation samples were stained with LIVE/DEAD Fixable Blue Dead Cell
497 Stain for 10 minutes at room temperature and surface stained with titrated amounts of anti-CD19,
498 anti-CD14, anti-CD16, anti-CD56, anti-CD4, anti-CD8, anti-CCR7 and anti-CD45RA for 20
499 minutes at room temperature. Cells were washed in FACS Buffer (PBS + 2% FBS), and fixed and
500 permeabilized (Cytofix/Cytoperm, BD Biosciences) for 20 minutes at room temperature.
501 Following fixation, cells were washed with Perm/Wash buffer (BD Biosciences) and stained
502 intracellularly with anti-CD3, anti-CD154, anti-CD69, anti-IFNg, anti-IL-2 and anti-TNF for 20
503 minutes at room temperature. Cells were subsequently washed with Perm/Wash buffer and fixed
504 with 1% paraformaldehyde. Data were acquired on a modified BD FACSymphony and analyzed
505 using FlowJo software (version 10.7.1). Cytokine frequencies were background subtracted and
506 negative values were set to zero.

507 Synthetic peptides (>75% purity by HPLC; 15 amino acids in length overlapping by 11
508 amino acids) were synthesized by GenScript. To measure T cell responses to the full-length WA-
509 1 Spike glycoprotein (YP_009724390.1), 2 peptide pools were utilized, Spike pool A (peptides 1-
510 160; residues 1-651) and Spike pool B (peptides 161-316; residues 641-1273) (Table S8).
511 Peptides were 15 amino acids in length and overlapped by 11 amino acids. Spike pool A
512 contained peptides for both D614 and the G614 mutation. Responses to full-length Spike were
513 calculated by summing the responses to both pools after background subtraction. Select peptide
514 pools were used to measure T cell responses to mutated regions of the Spike glycoproteins of
515 the Alpha, Beta and Gamma SARS-CoV-2 variants along with control pools corresponding to the
516 same regions within the WA-1 Spike glycoprotein (Table S9).
517

518 **Epitope mapping by Surface Plasmon Resonance (SPR)**

519 Serum epitope mapping competition assays were performed, as previously described (*47,*
520 *48*), using the Biacore 8K+ surface plasmon resonance system (Cytiva). Anti-histidine antibody
521 was immobilized on Series S Sensor Chip CM5 (Cytiva) through primary amine coupling using a
522 His capture kit (Cytiva). Following this, his-tagged SARS-CoV-2 S protein containing 2 proline
523 stabilization mutations (S-2P) was captured on the active sensor surface.

524 Human IgG monoclonal antibodies (mAb) used for these analyses include: B1-182, CB6,
525 A20-29.1, A19-46.1, LY-COV555, A19-61.1, S309, A23-97.1, A19-30.1, A23-80.1, and CR3022.
526 Either competitor or negative control mAb was injected over both active and reference surfaces.
527 Human sera were then flowed over both active and reference sensor surfaces, at a dilution of
528 1:50. Following the association phase, active and reference sensor surfaces were regenerated
529 between each analysis cycle.

530 Prior to analysis, sensorgrams were aligned to Y (Response Units) = 0, using Biacore 8K
531 Insights Evaluation Software (Cytiva), at the beginning of the serum association phase. Relative
532 "analyte binding late" report points (RU) were collected and used to calculate percent competition
533 (% C) using the following formula: % C = [1 – (100 * ((RU in presence of competitor mAb) / (RU
534 in presence of negative control mAb))]. Results are reported as percent competition and statistical
535 analysis was performed using unpaired, two-tailed t-test (Graphpad Prism v.8.3.1). All assays
536 were performed in duplicate and averaged.
537
538 **Production of antigen-specific probes**
539 Biotinylated probes for S-2P, NTD and RBD were produced as described previously (*77,*
540 *78*). Briefly, single-chain Fc and AVI-tagged proteins were expressed transiently for 6 days. After
541 harvest, the soluble proteins were purified and biotinylated in a single protein A column followed
542 by final purification on a Superdex 200 16/600 gel filtration column. Biotinylated proteins were
543 then conjugated to fluorescent streptavidin.
544
545 **Antigen-specific B cell sorting**
546 PBMC vials containing approximately 10^7 cells were thawed and stained with Live/Dead
547 Fixable Blue Dead Cell Stain Kit (Invitrogen, cat# L23105) for 10 min at room temperature,
548 followed by incubation for 20 min with the staining cocktail consisting of antibodies and probes.
549 The antibodies used in the staining cocktail were: CD8-BV510 (Biolegend, clone RPA-T8, cat#
550 301048), CD56-BV510 (Biolegend, clone HCD56, cat# 318340), CD14-BV510 (Biolegend, clone
551 M5E2, cat# 301842), CD16-BUV496 (BD Biosciences, clone 3G8, cat# 612944), CD3-APC-Cy7
552 (BD Biosciences, clone SP34-2, cat# 557757), CD19-PECy7 (Beckmann Coulter, clone J3-119,
553 cat# IM36284), CD20 (BD Biosciences, clone 2H7, cat# 564917), IgG-FITC (BD Biosciences,
554 clone G18-145, cat# 555786), IgA-FITC (Miltenyi Biotech, clone IS11-8E10, cat# 130-114-001)
555 and IgM-PECF594 (BD Biosciences, clone G20-127, cat# 562539). For each variant, a set of two
556 spike probes S-2P-APC and S-2P-BUV737, in addition to RBD-BV421 and NTD-BV711 were
557 included in the staining cocktail for flow cytometry sorting.
558 For RATP-Ig, single-cells were sorted in 96-well plates containing 5 µL of TCL buffer
559 (Qiagen) with 1% β-mercaptoethanol according to the gating strategy shown in Fig. S2B. Samples
560 sorted for 10x Genomics single-cell RNAseq were individually labelled with an oligonucleotide-
561 linked hashing antibody (Totalseq-C, Biolegend) in addition to the staining cocktail and sorted into
562 a single tube according to the gating strategy shown in Fig. S2B. All cell sorts were performed

563 using a BD FACSAria II instrument (BD Biosciences). Frequency of antigen-specific B cells were
564 analyzed using FlowJo 10.8.1 (BD Biosciences).
565
566 **Monoclonal antibody isolation and characterization by RATP-Ig**
567 **cDNA synthesis**: Variable heavy and light chains were synthesized using a modified
568 SMARTSeq-V4 protocol by 5' RACE. Single-cell RNA was first purified with RNAclean beads
569 (Beckman Coulter). cDNA was then synthesized using 5' RACE reverse-transcription, adding
570 distinct 3' and 5' template switch oligo adapters to total cDNA. cDNA was subsequently amplified
571 with TSO_FWD and TS_Oligo_2_REV primers. Excess oligos and dNTPs were removed from
572 amplified cDNA with EXO-CIP cleanup kit (New England BioLabs).
573 **Immunoglobulin enrichment and sequencing**: Heavy and light chain variable regions were
574 enriched by amplifying cDNA with TSO_FWD and IgA/IgG_REV or IgK/IgL_REV primer pools. An
575 aliquot of enriched product was used to prepare Nextera libraries with Unique Dual Indices
576 (Illumina) and sequenced using 2x150 paired-end reads on an Illumina MiSeq. Separate aliquots
577 were used for IG production; RATP-Ig is a modular system and can produce single combined or
578 separate HC/LC cassettes.
579 **Cassette fragment synthesis**: Final cassettes include CMV, and HC/LC-TBGH polyA fragments.
580 To isolate these fragments, amplicons were first synthesized by PCR. PCR products were run on
581 a 1% agarose gel and fragments of the correct length were extracted with Thermo gel extraction
582 and PCR cleanup kit (ThermoFisher Scientific). Gel-extracted products were digested with DpnI
583 (New England Biolabs) to further remove any possible contaminating plasmid. These fragment
584 templates were then further amplified to create final stocks of cassette fragments.
585 **Cassette assembly**: Enriched variable regions were assembled into linear expression cassettes
586 in two sequential ligation reactions. The first reaction assembles CMV-TSO, TSO-V-LC, and KC-
587 IRES fragments into part 1 and IRES-TSO, TSO-V-HC, and IgGC-TBGH fragments into part 2
588 using NEBuilder HIFI DNA Assembly Mastermix (New England BioLabs). Following reaction 1,
589 parts 1 and 2 were combined into a single reaction 2 and ligated into a single cassette.
590 Separate cassettes: Enriched variable regions were assembled into linear expression
591 cassettes by ligating CMV-TSO, TSO-V-C, and C-TBGH fragments using NEBuilder HIFI DNA
592 Assembly Mastermix (New England BioLabs). Assembled cassettes were amplified using
593 CMV_FWD and TBGH_REV primers. Amplified linear DNA cassettes encoding monoclonal heavy
594 and light chain genes were co-transfected into Expi293 cells in 96-well deep-well plates using the
595 Expi293 Transfection Kit (ThermoFisher Scientific) according to the manufacturer's protocol.

596 Microtiter cultures were incubated at 37 degrees and 8% CO_2 with shaking at 1100 RPM for 5-7
597 days before supernatants were clarified by centrifugation and harvested.
598
599 **Droplet-based single cell isolation and sequencing**
600 Antigen-specific memory B cells were sorted as described above. Cells from two separate
601 sorts were pooled in a single suspension and loaded on the 10x Genomics Chromium instrument
602 with reagents from the Next GEM Single Cell 5' Kit v1.1 following the manufacturer's protocol to
603 generate total cDNA. Heavy and light chains were amplified from the cDNA using custom 3'
604 primers specific for IgG, IgA, IgK or IgL with the addition of Illumina sequences (*79*). The Illumina-
605 ready libraries were sequenced using 2x300 paired-end reads on an Illumina MiSeq. Hashing
606 oligonucleotides were amplified and sequenced from the total cDNA according to the 10x
607 Genomics protocol.
608
609 **V(D)J sequence analysis**
610 For cells processed via RATP-Ig, reads were demultiplexed using a custom script and
611 candidate V(D)J sequences were generated using BALDR (*80*) and filtered for quality using a
612 custom script. The resulting sequences were annotated using SONAR v4.2 (*81*) in single-cell
613 mode.
614 For cells processed via the 10x Genomics Chromium device, reads from the hashing
615 libraries were processed using cellranger (10x Genomics). The resulting count matrix was
616 imported into Seurat (*82*) and the sample of origin called using the HTODemux function. Paired-
617 end reads from V(D)J libraries were merged and annotated using SONAR in single-cell mode with
618 UMI detection and processing.
619 For all datasets, nonproductive rearrangements were discarded, as were any cells with
620 more than one productive heavy or light chain. Cells with an unpaired heavy or light chain were
621 included in calculations of SHM and gene usage statistics, but were excluded from assessments
622 of clonality and determination of public clones. Public clones were determined by using the
623 clusterfast algorithm in vsearch (*83*) to cluster CDR H3 amino acid sequences at 80% identity.
624 Where relevant, all clonally related B cells in a single individual were included in a public clone,
625 even if not all were directly clustered together in the vsearch analysis.
626
627 **Supplementary Materials:**
628 **Fig. S1:** Additional serology and epitope mapping data. **A)** Antibody binding titers against multiple
629 variants assessed by cell surface binding assay; **B)** Structural schematic of spike protein showing

630 epitopes from monoclonal antibodies used for RBD epitope mapping by competition assay; **C)**
631 Epitope mapping of Beta-infected individuals on WA1, Beta and Delta spike proteins; **D)** Epitope
632 mapping of Gamma-infected individuals on WA1, Beta and Delta spike proteins; **E)** Gating
633 strategy for T cell response analysis.
634 **Fig. S2:** Antigen-specific B cell sorting. (**A**) Arrows indicate probes used for sorting antigen-
635 specific B cells from each group of convalescent individuals. The individual marked with a star
636 was used for both RATP-Ig and total BCR repertoire sequencing. (**B**) Flow cytometry
637 representative plots and gating strategies for B cell sorting and analysis; final sort gates are shown
638 in blue.
639 **Fig. S3**: SARS-CoV-2-specific light chain V gene usage frequencies. (A) Kappa and (B) Lambda
640 chain V gene repertoire analysis by infecting variant, with WA1, Beta and Gamma shown in grey,
641 orange and blue, respectively, and data from pre-pandemic controls in yellow. The x-axis shows
642 all germline genes used; the y-axis represents the percent of individual gene usage. Stars indicate
643 genes with at least one significant difference between groups; pairwise comparisons using the
644 Dunn test are in Table S7.
645
646 **Table S1:** Details of the study cohort.
647 **Table S2:** Serum epitope competition
648 **Table S3**: Heatmaps of complete RATP-Ig ELISA results for SAV1. Values are reported as
649 absorbance at 450nm wavelength.
650 **Table S4**: Heatmaps of complete RATP-Ig ELISA results for SAV3. Values are reported as
651 absorbance at 450nm wavelength.
652 **Table S5**: Heatmaps of complete RATP-Ig ELISA results for A49. Values are reported as
653 absorbance at 450nm wavelength.
654 **Table S6:** Sample recovery from 10x Genomics-based single cell isolation and sequencing.
655 **Table S7:** Significant differences in gene-usage. For genes with a significant difference detected
656 by the Kruskal-Wallis test (Figs. 4B and S3), the Dunn test was used to find significant pairwise
657 difference. P values were adjusted for multiple testing using the Benjami-Hochberg procedure.
658 **Table S8:** Sequences of peptides included in Spike pools A and B used for T cell stimulation.
659 Highlighted peptides did not meet >75% purity and were not included in the pool.
660 **Table S9:** Sequences of peptides included in selected peptide pools for each variant used for T
661 cell stimulation.
662
663

References and Notes

1. WHO, in *Tracking SARS-CoV-2 variants,* https://www.who.int/en/activities/tracking-SARS-CoV-2-variants, Ed. (2022).
2. B. Korber, W. M. Fischer, S. Gnanakaran, H. Yoon, J. Theiler, W. Abfalterer, N. Hengartner, E. E. Giorgi, T. Bhattacharya, B. Foley, K. M. Hastie, M. D. Parker, D. G. Partridge, C. M. Evans, T. M. Freeman, T. I. de Silva, C.-G. G. Sheffield, C. McDanal, L. G. Perez, H. Tang, A. Moon-Walker, S. P. Whelan, C. C. LaBranche, E. O. Saphire, D. C. Montefiori, Tracking Changes in SARS-CoV-2 Spike: Evidence that D614G Increases Infectivity of the COVID-19 Virus. *Cell* **182**, 812-827 e819 (2020).
3. D. Weissman, M. G. Alameh, T. de Silva, P. Collini, H. Hornsby, R. Brown, C. C. LaBranche, R. J. Edwards, L. Sutherland, S. Santra, K. Mansouri, S. Gobeil, C. McDanal, N. Pardi, N. Hengartner, P. J. C. Lin, Y. Tam, P. A. Shaw, M. G. Lewis, C. Boesler, U. Sahin, P. Acharya, B. F. Haynes, B. Korber, D. C. Montefiori, D614G Spike Mutation Increases SARS CoV-2 Susceptibility to Neutralization. *Cell Host Microbe* **29**, 23-31 e24 (2021).
4. Y. Weisblum, F. Schmidt, F. Zhang, J. DaSilva, D. Poston, J. C. Lorenzi, F. Muecksch, M. Rutkowska, H. H. Hoffmann, E. Michailidis, C. Gaebler, M. Agudelo, A. Cho, Z. Wang, A. Gazumyan, M. Cipolla, L. Luchsinger, C. D. Hillyer, M. Caskey, D. F. Robbiani, C. M. Rice, M. C. Nussenzweig, T. Hatziioannou, P. D. Bieniasz, Escape from neutralizing antibodies by SARS-CoV-2 spike protein variants. *Elife* **9**, (2020).
5. F. Schmidt, Y. Weisblum, M. Rutkowska, D. Poston, J. DaSilva, F. Zhang, E. Bednarski, A. Cho, D. J. Schaefer-Babajew, C. Gaebler, M. Caskey, M. C. Nussenzweig, T. Hatziioannou, P. D. Bieniasz, High genetic barrier to SARS-CoV-2 polyclonal neutralizing antibody escape. *Nature* **600**, 512-516 (2021).
6. W. Dejnirattisai, D. Zhou, P. Supasa, C. Liu, A. J. Mentzer, H. M. Ginn, Y. Zhao, H. M. E. Duyvesteyn, A. Tuekprakhon, R. Nutalai, B. Wang, C. Lopez-Camacho, J. Slon-Campos, T. S. Walter, D. Skelly, S. A. Costa Clemens, F. G. Naveca, V. Nascimento, F. Nascimento, C. Fernandes da Costa, P. C. Resende, A. Pauvolid-Correa, M. M. Siqueira, C. Dold, R. Levin, T. Dong, A. J. Pollard, J. C. Knight, D. Crook, T. Lambe, E. Clutterbuck, S. Bibi, A. Flaxman, M. Bittaye, S. Belij-Rammerstorfer, S. C. Gilbert, M. W. Carroll, P. Klenerman, E. Barnes, S. J. Dunachie, N. G. Paterson, M. A. Williams, D. R. Hall, R. J. G. Hulswit, T. A. Bowden, E. E. Fry, J. Mongkolsapaya, J. Ren, D. I. Stuart, G. R. Screaton, Antibody evasion by the P.1 strain of SARS-CoV-2. *Cell* **184**, 2939-2954 e2939 (2021).
7. W. Dejnirattisai, J. Huo, D. Zhou, J. Zahradnik, P. Supasa, C. Liu, H. M. E. Duyvesteyn, H. M. Ginn, A. J. Mentzer, A. Tuekprakhon, R. Nutalai, B. Wang, A. Dijokaite, S. Khan, O. Avinoam, M. Bahar, D. Skelly, S. Adele, S. A. Johnson, A. Amini, T. G. Ritter, C. Mason, C. Dold, D. Pan, S. Assadi, A. Bellass, N. Omo-Dare, D. Koeckerling, A. Flaxman, D. Jenkin, P. K. Aley, M. Voysey, S. A. Costa Clemens, F. G. Naveca, V. Nascimento, F. Nascimento, C. Fernandes da Costa, P. C. Resende, A. Pauvolid-Correa, M. M. Siqueira, V. Baillie, N. Serafin, G. Kwatra, K. Da Silva, S. A. Madhi, M. C. Nunes, T. Malik, P. J. M. Openshaw, J. K. Baillie, M. G. Semple, A. R. Townsend, K. A. Huang, T. K. Tan, M. W. Carroll, P. Klenerman, E. Barnes, S. J. Dunachie, B. Constantinides, H. Webster, D. Crook, A. J. Pollard, T. Lambe, O. Consortium, I. C. Consortium, N. G. Paterson, M. A. Williams, D. R. Hall, E. E. Fry, J. Mongkolsapaya, J. Ren, G. Schreiber, D. I. Stuart, G. R.

Screaton, SARS-CoV-2 Omicron-B.1.1.529 leads to widespread escape from neutralizing antibody responses. *Cell* **185**, 467-484 e415 (2022).

8. F. Amanat, M. Thapa, T. Lei, S. M. S. Ahmed, D. C. Adelsberg, J. M. Carreno, S. Strohmeier, A. J. Schmitz, S. Zafar, J. Q. Zhou, W. Rijnink, H. Alshammary, N. Borcherding, A. G. Reiche, K. Srivastava, E. M. Sordillo, H. van Bakel, I. Personalized Virology, J. S. Turner, G. Bajic, V. Simon, A. H. Ellebedy, F. Krammer, SARS-CoV-2 mRNA vaccination induces functionally diverse antibodies to NTD, RBD, and S2. *Cell* **184**, 3936-3948 e3910 (2021).
9. T. N. Starr, A. J. Greaney, S. K. Hilton, D. Ellis, K. H. D. Crawford, A. S. Dingens, M. J. Navarro, J. E. Bowen, M. A. Tortorici, A. C. Walls, N. P. King, D. Veesler, J. D. Bloom, Deep Mutational Scanning of SARS-CoV-2 Receptor Binding Domain Reveals Constraints on Folding and ACE2 Binding. *Cell* **182**, 1295-1310 e1220 (2020).
10. M. Kandeel, M. E. M. Mohamed, H. M. Abd El-Lateef, K. N. Venugopala, H. S. El-Beltagi, Omicron variant genome evolution and phylogenetics. *J Med Virol* **94**, 1627-1632 (2022).
11. E. Boehm, I. Kronig, R. A. Neher, I. Eckerle, P. Vetter, L. Kaiser, D. Geneva Centre for Emerging Viral, Novel SARS-CoV-2 variants: the pandemics within the pandemic. *Clin Microbiol Infect* **27**, 1109-1117 (2021).
12. P. Wang, M. S. Nair, L. Liu, S. Iketani, Y. Luo, Y. Guo, M. Wang, J. Yu, B. Zhang, P. D. Kwong, B. S. Graham, J. R. Mascola, J. Y. Chang, M. T. Yin, M. Sobieszczyk, C. A. Kyratsous, L. Shapiro, Z. Sheng, Y. Huang, D. D. Ho, Antibody resistance of SARS-CoV-2 variants B.1.351 and B.1.1.7. *Nature* **593**, 130-135 (2021).
13. L. Wang, T. Zhou, Y. Zhang, E. S. Yang, C. A. Schramm, W. Shi, A. Pegu, O. K. Oloniniyi, A. R. Henry, S. Darko, S. R. Narpala, C. Hatcher, D. R. Martinez, Y. Tsybovsky, E. Phung, O. M. Abiona, A. Antia, E. M. Cale, L. A. Chang, M. Choe, K. S. Corbett, R. L. Davis, A. T. DiPiazza, I. J. Gordon, S. H. Hait, T. Hermanus, P. Kgagudi, F. Laboune, K. Leung, T. Liu, R. D. Mason, A. F. Nazzari, L. Novik, S. O'Connell, S. O'Dell, A. S. Olia, S. D. Schmidt, T. Stephens, C. D. Stringham, C. A. Talana, I. T. Teng, D. A. Wagner, A. T. Widge, B. Zhang, M. Roederer, J. E. Ledgerwood, T. J. Ruckwardt, M. R. Gaudinski, P. L. Moore, N. A. Doria-Rose, R. S. Baric, B. S. Graham, A. B. McDermott, D. C. Douek, P. D. Kwong, J. R. Mascola, N. J. Sullivan, J. Misasi, Ultrapotent antibodies against diverse and highly transmissible SARS-CoV-2 variants. *Science* **373**, (2021).
14. S. Changrob, Y. Fu, J. J. Guthmiller, P. J. Halfmann, L. Li, C. T. Stamper, H. L. Dugan, M. Accola, W. Rehrauer, N. Y. Zheng, M. Huang, J. Wang, S. A. Erickson, H. A. Utset, H. M. Graves, F. Amanat, D. N. Sather, F. Krammer, Y. Kawaoka, P. C. Wilson, Cross-Neutralization of Emerging SARS-CoV-2 Variants of Concern by Antibodies Targeting Distinct Epitopes on Spike. *mBio* **12**, e0297521 (2021).
15. L. Piccoli, Y. J. Park, M. A. Tortorici, N. Czudnochowski, A. C. Walls, M. Beltramello, C. Silacci-Fregni, D. Pinto, L. E. Rosen, J. E. Bowen, O. J. Acton, S. Jaconi, B. Guarino, A. Minola, F. Zatta, N. Sprugasci, J. Bassi, A. Peter, A. De Marco, J. C. Nix, F. Mele, S. Jovic, B. F. Rodriguez, S. V. Gupta, F. Jin, G. Piumatti, G. Lo Presti, A. F. Pellanda, M. Biggiogero, M. Tarkowski, M. S. Pizzuto, E. Cameroni, C. Havenar-Daughton, M. Smithey, D. Hong, V. Lepori, E. Albanese, A. Ceschi, E. Bernasconi, L. Elzi, P. Ferrari, C. Garzoni, A. Riva, G. Snell, F. Sallusto, K. Fink, H. W. Virgin, A. Lanzavecchia, D. Corti, D. Veesler, Mapping Neutralizing and Immunodominant Sites on the SARS-CoV-2 Spike Receptor-Binding Domain by Structure-Guided High-Resolution Serology. *Cell* **183**, 1024-1042 e1021 (2020).

755 16. V. Dussupt, R. S. Sankhala, L. Mendez-Rivera, S. M. Townsley, F. Schmidt, L. Wieczorek,
756 K. G. Lal, G. C. Donofrio, U. Tran, N. D. Jackson, W. I. Zaky, M. Zemil, S. R. Tritsch, W.
757 H. Chen, E. J. Martinez, A. Ahmed, M. Choe, W. C. Chang, A. Hajduczki, N. Jian, C. E.
758 Peterson, P. A. Rees, M. Rutkowska, B. M. Slike, C. N. Selverian, I. Swafford, I. T. Teng,
759 P. V. Thomas, T. Zhou, C. J. Smith, J. R. Currier, P. D. Kwong, M. Rolland, E. Davidson,
760 B. J. Doranz, C. N. Mores, T. Hatziioannou, W. W. Reiley, P. D. Bieniasz, D. Paquin-
761 Proulx, G. D. Gromowski, V. R. Polonis, N. L. Michael, K. Modjarrad, M. G. Joyce, S. J.
762 Krebs, Low-dose in vivo protection and neutralization across SARS-CoV-2 variants by
763 monoclonal antibody combinations. *Nat Immunol* **22**, 1503-1514 (2021).
764 17. G. Beaudoin-Bussieres, Y. Chen, I. Ullah, J. Prevost, W. D. Tolbert, K. Symmes, S. Ding,
765 M. Benlarbi, S. Y. Gong, A. Tauzin, R. Gasser, D. Chatterjee, D. Vezina, G. Goyette, J.
766 Richard, F. Zhou, L. Stamatatos, A. T. McGuire, H. Charest, M. Roger, E. Pozharski, P.
767 Kumar, W. Mothes, P. D. Uchil, M. Pazgier, A. Finzi, A Fc-enhanced NTD-binding non-
768 neutralizing antibody delays virus spread and synergizes with a nAb to protect mice from
769 lethal SARS-CoV-2 infection. *Cell Rep* **38**, 110368 (2022).
770 18. D. Geers, M. C. Shamier, S. Bogers, G. den Hartog, L. Gommers, N. N. Nieuwkoop, K. S.
771 Schmitz, L. C. Rijsbergen, J. A. T. van Osch, E. Dijkhuizen, G. Smits, A. Comvalius, D.
772 van Mourik, T. G. Caniels, M. J. van Gils, R. W. Sanders, B. B. Oude Munnink, R.
773 Molenkamp, H. J. de Jager, B. L. Haagmans, R. L. de Swart, M. P. G. Koopmans, R. S.
774 van Binnendijk, R. D. de Vries, C. H. GeurtsvanKessel, SARS-CoV-2 variants of concern
775 partially escape humoral but not T-cell responses in COVID-19 convalescent donors and
776 vaccinees. *Sci Immunol* **6**, (2021).
777 19. A. Tarke, J. Sidney, N. Methot, E. D. Yu, Y. Zhang, J. M. Dan, B. Goodwin, P. Rubiro, A.
778 Sutherland, E. Wang, A. Frazier, S. I. Ramirez, S. A. Rawlings, D. M. Smith, R. da Silva
779 Antunes, B. Peters, R. H. Scheuermann, D. Weiskopf, S. Crotty, A. Grifoni, A. Sette,
780 Impact of SARS-CoV-2 variants on the total CD4(+) and CD8(+) T cell reactivity in
781 infected or vaccinated individuals. *Cell Rep Med* **2**, 100355 (2021).
782 20. Y. Gao, C. Cai, A. Grifoni, T. R. Muller, J. Niessl, A. Olofsson, M. Humbert, L. Hansson,
783 A. Osterborg, P. Bergman, P. Chen, A. Olsson, J. K. Sandberg, D. Weiskopf, D. A. Price,
784 H. G. Ljunggren, A. C. Karlsson, A. Sette, S. Aleman, M. Buggert, Ancestral SARS-CoV-
785 2-specific T cells cross-recognize the Omicron variant. *Nat Med*, (2022).
786 21. A. D. Redd, A. Nardin, H. Kared, E. M. Bloch, A. Pekosz, O. Laeyendecker, B. Abel, M.
787 Fehlings, T. C. Quinn, A. A. R. Tobian, CD8+ T-Cell Responses in COVID-19
788 Convalescent Individuals Target Conserved Epitopes From Multiple Prominent SARS-
789 CoV-2 Circulating Variants. *Open Forum Infect Dis* **8**, ofab143 (2021).
790 22. A. Tarke, C. H. Coelho, Z. Zhang, J. M. Dan, E. D. Yu, N. Methot, N. I. Bloom, B.
791 Goodwin, E. Phillips, S. Mallal, J. Sidney, G. Filaci, D. Weiskopf, R. da Silva Antunes, S.
792 Crotty, A. Grifoni, A. Sette, SARS-CoV-2 vaccination induces immunological T cell
793 memory able to cross-recognize variants from Alpha to Omicron. *Cell* **185**, 847-859 e811
794 (2022).
795 23. C. O. Barnes, C. A. Jette, M. E. Abernathy, K. A. Dam, S. R. Esswein, H. B. Gristick, A.
796 G. Malyutin, N. G. Sharaf, K. E. Huey-Tubman, Y. E. Lee, D. F. Robbiani, M. C.
797 Nussenzweig, A. P. West, Jr., P. J. Bjorkman, SARS-CoV-2 neutralizing antibody
798 structures inform therapeutic strategies. *Nature* **588**, 682-687 (2020).
799 24. H. L. Dugan, C. T. Stamper, L. Li, S. Changrob, N. W. Asby, P. J. Halfmann, N. Y. Zheng,
800 M. Huang, D. G. Shaw, M. S. Cobb, S. A. Erickson, J. J. Guthmiller, O. Stovicek, J. Wang,

E. S. Winkler, M. L. Madariaga, K. Shanmugarajah, M. O. Jansen, F. Amanat, I. Stewart, H. A. Utset, J. Huang, C. A. Nelson, Y. N. Dai, P. D. Hall, R. P. Jedrzejczak, A. Joachimiak, F. Krammer, M. S. Diamond, D. H. Fremont, Y. Kawaoka, P. C. Wilson, Profiling B cell immunodominance after SARS-CoV-2 infection reveals antibody evolution to non-neutralizing viral targets. *Immunity* **54**, 1290-1303 e1297 (2021).

25. P. Tong, A. Gautam, I. W. Windsor, M. Travers, Y. Chen, N. Garcia, N. B. Whiteman, L. G. A. McKay, N. Storm, L. E. Malsick, A. N. Honko, F. J. N. Lelis, S. Habibi, S. Jenni, Y. Cai, L. J. Rennick, W. P. Duprex, K. R. McCarthy, C. L. Lavine, T. Zuo, J. Lin, A. Zuiani, J. Feldman, E. A. MacDonald, B. M. Hauser, A. Griffths, M. S. Seaman, A. G. Schmidt, B. Chen, D. Neuberg, G. Bajic, S. C. Harrison, D. R. Wesemann, Memory B cell repertoire for recognition of evolving SARS-CoV-2 spike. *Cell* **184**, 4969-4980 e4915 (2021).
26. A. J. Greaney, T. N. Starr, P. Gilchuk, S. J. Zost, E. Binshtein, A. N. Loes, S. K. Hilton, J. Huddleston, R. Eguia, K. H. D. Crawford, A. S. Dingens, R. S. Nargi, R. E. Sutton, N. Suryadevara, P. W. Rothlauf, Z. Liu, S. P. J. Whelan, R. H. Carnahan, J. E. Crowe, Jr., J. D. Bloom, Complete Mapping of Mutations to the SARS-CoV-2 Spike Receptor-Binding Domain that Escape Antibody Recognition. *Cell Host Microbe* **29**, 44-57 e49 (2021).
27. M. McCallum, A. De Marco, F. A. Lempp, M. A. Tortorici, D. Pinto, A. C. Walls, M. Beltramello, A. Chen, Z. Liu, F. Zatta, S. Zepeda, J. di Iulio, J. E. Bowen, M. Montiel-Ruiz, J. Zhou, L. E. Rosen, S. Bianchi, B. Guarino, C. S. Fregni, R. Abdelnabi, S. C. Foo, P. W. Rothlauf, L. M. Bloyet, F. Benigni, E. Cameroni, J. Neyts, A. Riva, G. Snell, A. Telenti, S. P. J. Whelan, H. W. Virgin, D. Corti, M. S. Pizzuto, D. Veesler, N-terminal domain antigenic mapping reveals a site of vulnerability for SARS-CoV-2. *Cell* **184**, 2332-2347 e2316 (2021).
28. P. J. M. Brouwer, T. G. Caniels, K. van der Straten, J. L. Snitselaar, Y. Aldon, S. Bangaru, J. L. Torres, N. M. A. Okba, M. Claireaux, G. Kerster, A. E. H. Bentlage, M. M. van Haaren, D. Guerra, J. A. Burger, E. E. Schermer, K. D. Verheul, N. van der Velde, A. van der Kooi, J. van Schooten, M. J. van Breemen, T. P. L. Bijl, K. Sliepen, A. Aartse, R. Derking, I. Bontjer, N. A. Kootstra, W. J. Wiersinga, G. Vidarsson, B. L. Haagmans, A. B. Ward, G. J. de Bree, R. W. Sanders, M. J. van Gils, Potent neutralizing antibodies from COVID-19 patients define multiple targets of vulnerability. *Science* **369**, 643-650 (2020).
29. W. Dejnirattisai, D. Zhou, H. M. Ginn, H. M. E. Duyvesteyn, P. Supasa, J. B. Case, Y. Zhao, T. S. Walter, A. J. Mentzer, C. Liu, B. Wang, G. C. Paesen, J. Slon-Campos, C. Lopez-Camacho, N. M. Kafai, A. L. Bailey, R. E. Chen, B. Ying, C. Thompson, J. Bolton, A. Fyfe, S. Gupta, T. K. Tan, J. Gilbert-Jaramillo, W. James, M. Knight, M. W. Carroll, D. Skelly, C. Dold, Y. Peng, R. Levin, T. Dong, A. J. Pollard, J. C. Knight, P. Klenerman, N. Temperton, D. R. Hall, M. A. Williams, N. G. Paterson, F. K. R. Bertram, C. A. Siebert, D. K. Clare, A. Howe, J. Radecke, Y. Song, A. R. Townsend, K. A. Huang, E. E. Fry, J. Mongkolsapaya, M. S. Diamond, J. Ren, D. I. Stuart, G. R. Screaton, The antigenic anatomy of SARS-CoV-2 receptor binding domain. *Cell* **184**, 2183-2200 e2122 (2021).
30. G. Cerutti, Y. Guo, T. Zhou, J. Gorman, M. Lee, M. Rapp, E. R. Reddem, J. Yu, F. Bahna, J. Bimela, Y. Huang, P. S. Katsamba, L. Liu, M. S. Nair, R. Rawi, A. S. Olia, P. Wang, B. Zhang, G. Y. Chuang, D. D. Ho, Z. Sheng, P. D. Kwong, L. Shapiro, Potent SARS-CoV-2 neutralizing antibodies directed against spike N-terminal domain target a single supersite. *Cell Host Microbe* **29**, 819-833 e817 (2021).
31. L. Liu, P. Wang, M. S. Nair, J. Yu, M. Rapp, Q. Wang, Y. Luo, J. F. Chan, V. Sahi, A. Figueroa, X. V. Guo, G. Cerutti, J. Bimela, J. Gorman, T. Zhou, Z. Chen, K. Y. Yuen, P.

847 D. Kwong, J. G. Sodroski, M. T. Yin, Z. Sheng, Y. Huang, L. Shapiro, D. D. Ho, Potent
848 neutralizing antibodies against multiple epitopes on SARS-CoV-2 spike. *Nature* **584**, 450-
849 456 (2020).
850 32. J. D. Galson, S. Schaetzle, R. J. M. Bashford-Rogers, M. I. J. Raybould, A. Kovaltsuk, G.
851 J. Kilpatrick, R. Minter, D. K. Finch, J. Dias, L. K. James, G. Thomas, W. J. Lee, J. Betley,
852 O. Cavlan, A. Leech, C. M. Deane, J. Seoane, C. Caldas, D. J. Pennington, P. Pfeffer, J.
853 Osbourn, Deep Sequencing of B Cell Receptor Repertoires From COVID-19 Patients
854 Reveals Strong Convergent Immune Signatures. *Front Immunol* **11**, 605170 (2020).
855 33. M. Rapp, Y. Guo, E. R. Reddem, J. Yu, L. Liu, P. Wang, G. Cerutti, P. Katsamba, J. S.
856 Bimela, F. A. Bahna, S. M. Mannepalli, B. Zhang, P. D. Kwong, Y. Huang, D. D. Ho, L.
857 Shapiro, Z. Sheng, Modular basis for potent SARS-CoV-2 neutralization by a prevalent
858 VH1-2-derived antibody class. *Cell Rep* **35**, 108950 (2021).
859 34. S. J. Zost, P. Gilchuk, R. E. Chen, J. B. Case, J. X. Reidy, A. Trivette, R. S. Nargi, R. E.
860 Sutton, N. Suryadevara, E. C. Chen, E. Binshtein, S. Shrihari, M. Ostrowski, H. Y. Chu, J.
861 E. Didier, K. W. MacRenaris, T. Jones, S. Day, L. Myers, F. Eun-Hyung Lee, D. C.
862 Nguyen, I. Sanz, D. R. Martinez, P. W. Rothlauf, L. M. Bloyet, S. P. J. Whelan, R. S. Baric,
863 L. B. Thackray, M. S. Diamond, R. H. Carnahan, J. E. Crowe, Jr., Rapid isolation and
864 profiling of a diverse panel of human monoclonal antibodies targeting the SARS-CoV-2
865 spike protein. *Nat Med* **26**, 1422-1427 (2020).
866 35. Y. Cao, B. Su, X. Guo, W. Sun, Y. Deng, L. Bao, Q. Zhu, X. Zhang, Y. Zheng, C. Geng,
867 X. Chai, R. He, X. Li, Q. Lv, H. Zhu, W. Deng, Y. Xu, Y. Wang, L. Qiao, Y. Tan, L. Song,
868 G. Wang, X. Du, N. Gao, J. Liu, J. Xiao, X. D. Su, Z. Du, Y. Feng, C. Qin, C. Qin, R. Jin,
869 X. S. Xie, Potent Neutralizing Antibodies against SARS-CoV-2 Identified by High-
870 Throughput Single-Cell Sequencing of Convalescent Patients' B Cells. *Cell* **182**, 73-84 e16
871 (2020).
872 36. D. F. Robbiani, C. Gaebler, F. Muecksch, J. C. C. Lorenzi, Z. Wang, A. Cho, M. Agudelo,
873 C. O. Barnes, A. Gazumyan, S. Finkin, T. Hagglof, T. Y. Oliveira, C. Viant, A. Hurley, H.
874 H. Hoffmann, K. G. Millard, R. G. Kost, M. Cipolla, K. Gordon, F. Bianchini, S. T. Chen,
875 V. Ramos, R. Patel, J. Dizon, I. Shimeliovich, P. Mendoza, H. Hartweger, L. Nogueira, M.
876 Pack, J. Horowitz, F. Schmidt, Y. Weisblum, E. Michailidis, A. W. Ashbrook, E. Waltari,
877 J. E. Pak, K. E. Huey-Tubman, N. Koranda, P. R. Hoffman, A. P. West, Jr., C. M. Rice, T.
878 Hatziioannou, P. J. Bjorkman, P. D. Bieniasz, M. Caskey, M. C. Nussenzweig, Convergent
879 antibody responses to SARS-CoV-2 in convalescent individuals. *Nature* **584**, 437-442
880 (2020).
881 37. P. D. Kwong, J. R. Mascola, HIV-1 Vaccines Based on Antibody Identification, B Cell
882 Ontogeny, and Epitope Structure. *Immunity* **48**, 855-871 (2018).
883 38. M. Yuan, H. Liu, N. C. Wu, C. D. Lee, X. Zhu, F. Zhao, D. Huang, W. Yu, Y. Hua, H.
884 Tien, T. F. Rogers, E. Landais, D. Sok, J. G. Jardine, D. R. Burton, I. A. Wilson, Structural
885 basis of a shared antibody response to SARS-CoV-2. *Science* **369**, 1119-1123 (2020).
886 39. N. C. Wu, M. Yuan, H. Liu, C. D. Lee, X. Zhu, S. Bangaru, J. L. Torres, T. G. Caniels, P.
887 J. M. Brouwer, M. J. van Gils, R. W. Sanders, A. B. Ward, I. A. Wilson, An Alternative
888 Binding Mode of IGHV3-53 Antibodies to the SARS-CoV-2 Receptor Binding Domain.
889 *Cell Rep* **33**, 108274 (2020).
890 40. C. O. Barnes, A. P. West, Jr., K. E. Huey-Tubman, M. A. G. Hoffmann, N. G. Sharaf, P.
891 R. Hoffman, N. Koranda, H. B. Gristick, C. Gaebler, F. Muecksch, J. C. C. Lorenzi, S.
892 Finkin, T. Hagglof, A. Hurley, K. G. Millard, Y. Weisblum, F. Schmidt, T. Hatziioannou,

P. D. Bieniasz, M. Caskey, D. F. Robbiani, M. C. Nussenzweig, P. J. Bjorkman, Structures of Human Antibodies Bound to SARS-CoV-2 Spike Reveal Common Epitopes and Recurrent Features of Antibodies. *Cell* **182**, 828-842 e816 (2020).

41. J. Dong, S. J. Zost, A. J. Greaney, T. N. Starr, A. S. Dingens, E. C. Chen, R. E. Chen, J. B. Case, R. E. Sutton, P. Gilchuk, J. Rodriguez, E. Armstrong, C. Gainza, R. S. Nargi, E. Binshtein, X. Xie, X. Zhang, P. Y. Shi, J. Logue, S. Weston, M. E. McGrath, M. B. Frieman, T. Brady, K. M. Tuffy, H. Bright, Y. M. Loo, P. M. McTamney, M. T. Esser, R. H. Carnahan, M. S. Diamond, J. D. Bloom, J. E. Crowe, Jr., Genetic and structural basis for SARS-CoV-2 variant neutralization by a two-antibody cocktail. *Nat Microbiol* **6**, 1233-1244 (2021).
42. D. Zhou, W. Dejnirattisai, P. Supasa, C. Liu, A. J. Mentzer, H. M. Ginn, Y. Zhao, H. M. E. Duyvesteyn, A. Tuekprakhon, R. Nutalai, B. Wang, G. C. Paesen, C. Lopez-Camacho, J. Slon-Campos, B. Hallis, N. Coombes, K. Bewley, S. Charlton, T. S. Walter, D. Skelly, S. F. Lumley, C. Dold, R. Levin, T. Dong, A. J. Pollard, J. C. Knight, D. Crook, T. Lambe, E. Clutterbuck, S. Bibi, A. Flaxman, M. Bittaye, S. Belij-Rammerstorfer, S. Gilbert, W. James, M. W. Carroll, P. Klenerman, E. Barnes, S. J. Dunachie, E. E. Fry, J. Mongkolsapaya, J. Ren, D. I. Stuart, G. R. Screaton, Evidence of escape of SARS-CoV-2 variant B.1.351 from natural and vaccine-induced sera. *Cell* **184**, 2348-2361 e2346 (2021).
43. K. Vanshylla, V. Di Cristanziano, F. Kleipass, F. Dewald, P. Schommers, L. Gieselmann, H. Gruell, M. Schlotz, M. S. Ercanoglu, R. Stumpf, P. Mayer, M. Zehner, E. Heger, W. Johannis, C. Horn, I. Suarez, N. Jung, S. Salomon, K. A. Eberhardt, B. Gathof, G. Fatkenheuer, N. Pfeifer, R. Eggeling, M. Augustin, C. Lehmann, F. Klein, Kinetics and correlates of the neutralizing antibody response to SARS-CoV-2 infection in humans. *Cell Host Microbe* **29**, 917-929 e914 (2021).
44. T. Zhou, L. Wang, J. Misasi, A. Pegu, Y. Zhang, D. R. Harris, A. S. Olia, C. A. Talana, E. S. Yang, M. Chen, M. Choe, W. Shi, I. T. Teng, A. Creanga, C. Jenkins, K. Leung, T. Liu, E. D. Stancofski, T. Stephens, B. Zhang, Y. Tsybovsky, B. S. Graham, J. R. Mascola, N. J. Sullivan, P. D. Kwong, Structural basis for potent antibody neutralization of SARS-CoV-2 variants including B.1.1.529. *Science*, eabn8897 (2022).
45. T. Moyo-Gwete, M. Madzivhandila, Z. Makhado, F. Ayres, D. Mhlanga, B. Oosthuysen, B. E. Lambson, P. Kgagudi, H. Tegally, A. Iranzadeh, D. Doolabh, L. Tyers, L. R. Chinhoyi, M. Mennen, S. Skelem, G. Marais, C. K. Wibmer, J. N. Bhiman, V. Ueckermann, T. Rossouw, M. Boswell, T. de Oliveira, C. Williamson, W. A. Burgers, N. Ntusi, L. Morris, P. L. Moore, Cross-Reactive Neutralizing Antibody Responses Elicited by SARS-CoV-2 501Y.V2 (B.1.351). *N Engl J Med* **384**, 2161-2163 (2021).
46. C. Liu, H. M. Ginn, W. Dejnirattisai, P. Supasa, B. Wang, A. Tuekprakhon, R. Nutalai, D. Zhou, A. J. Mentzer, Y. Zhao, H. M. E. Duyvesteyn, C. Lopez-Camacho, J. Slon-Campos, T. S. Walter, D. Skelly, S. A. Johnson, T. G. Ritter, C. Mason, S. A. Costa Clemens, F. Gomes Naveca, V. Nascimento, F. Nascimento, C. Fernandes da Costa, P. C. Resende, A. Pauvolid-Correa, M. M. Siqueira, C. Dold, N. Temperton, T. Dong, A. J. Pollard, J. C. Knight, D. Crook, T. Lambe, E. Clutterbuck, S. Bibi, A. Flaxman, M. Bittaye, S. Belij-Rammerstorfer, S. C. Gilbert, T. Malik, M. W. Carroll, P. Klenerman, E. Barnes, S. J. Dunachie, V. Baillie, N. Serafin, Z. Ditse, K. Da Silva, N. G. Paterson, M. A. Williams, D. R. Hall, S. Madhi, M. C. Nunes, P. Goulder, E. E. Fry, J. Mongkolsapaya, J. Ren, D. I. Stuart, G. R. Screaton, Reduced neutralization of SARS-CoV-2 B.1.617 by vaccine and convalescent serum. *Cell* **184**, 4220-4236 e4213 (2021).

47. K. S. Corbett, M. Gagne, D. A. Wagner, O. C. S, S. R. Narpala, D. R. Flebbe, S. F. Andrew, R. L. Davis, B. Flynn, T. S. Johnston, C. D. Stringham, L. Lai, D. Valentin, A. Van Ry, Z. Flinchbaugh, A. P. Werner, J. I. Moliva, M. Sriparna, S. O'Dell, S. D. Schmidt, C. Tucker, A. Choi, M. Koch, K. W. Bock, M. Minai, B. M. Nagata, G. S. Alvarado, A. R. Henry, F. Laboune, C. A. Schramm, Y. Zhang, E. S. Yang, L. Wang, M. Choe, S. Boyoglu-Barnum, S. Wei, E. Lamb, S. T. Nurmukhambetova, S. J. Provost, M. M. Donaldson, J. Marquez, J. M. Todd, A. Cook, A. Dodson, A. Pekosz, E. Boritz, A. Ploquin, N. Doria-Rose, L. Pessaint, H. Andersen, K. E. Foulds, J. Misasi, K. Wu, A. Carfi, M. C. Nason, J. Mascola, I. N. Moore, D. K. Edwards, M. G. Lewis, M. S. Suthar, M. Roederer, A. McDermott, D. C. Douek, N. J. Sullivan, B. S. Graham, R. A. Seder, Protection against SARS-CoV-2 Beta variant in mRNA-1273 vaccine-boosted nonhuman primates. *Science* **374**, 1343-1353 (2021).

48. M. M. Gagne, J.I.; Foulds, K.E.; Andrew, S.F.; Flynn, B.J.; Werner, A.P.; Wagner, D.A.; Teng, I.-T.; Lin, B.C.; Moore, C.; Jean-Baptiste, N.; Carroll, R.; Foster, S.L.; Patel, M.; Ellis, M.; Edara, V.-V.; Maldonado, N.V.; Minai, M.; McCormick, L.; Honeycutt, C.C.; Nagata, B.M.; Bock, K.W.; Dulan, C.N.M.; Cordon, J.; Flebbe, D.R.; Todd, J.-P.M.; McCarthy, E.; Pessaint, L.; Van Ry, A.; Narvaez, B.; Valentin, D.; Cook, A.; Dodson, A.; Steingrebe, K.; Nurmukhambetova, S.T.;, S. H. Godbole, A.R.; Laboune, F.; Roberts-Torres, J.; Lorang, C.G.; Amin, S.; Trost, J.; Naisan, M.; Basappa, M.; Willis, J.; Wang, L.; Shi, W.; Doria-Rose, N.A.; Zhang, Y.; Yang, E.S.; Leung, K.; O'Dell, S.; Schmidt, S.D.; Olia, A.S.; Liu, C.; Harris, D.R.; Chuang, G.-Y.; Stewart-Jones, G.; Renzi, I.; Lai, Y.- T.; Malinowski, A.; Wu, K.; Mascola, J.R.; Carfi, A.; Kwong, P.D.; Edwards, D.K.; Lewis, M.G.; Andersen, H.; Corbett, K.S.; Nason, M.C.; McDermott, A.B.; Suthar, M.S.; Moore, I.N.; Roederer, M.; Sullivan, N.J.; Douek, D.C.; Seder, R.A., mRNA-1273 or mRNA-Omicron boost in vaccinated macaques elicits comparable B cell expansion, neutralizing antibodies and protection against Omicron. *Cell*, (2022).

49. D. Li, R. J. Edwards, K. Manne, D. R. Martinez, A. Schafer, S. M. Alam, K. Wiehe, X. Lu, R. Parks, L. L. Sutherland, T. H. Oguin, 3rd, C. McDanal, L. G. Perez, K. Mansouri, S. M. C. Gobeil, K. Janowska, V. Stalls, M. Kopp, F. Cai, E. Lee, A. Foulger, G. E. Hernandez, A. Sanzone, K. Tilahun, C. Jiang, L. V. Tse, K. W. Bock, M. Minai, B. M. Nagata, K. Cronin, V. Gee-Lai, M. Deyton, M. Barr, T. Von Holle, A. N. Macintyre, E. Stover, J. Feldman, B. M. Hauser, T. M. Caradonna, T. D. Scobey, W. Rountree, Y. Wang, M. A. Moody, D. W. Cain, C. T. DeMarco, T. N. Denny, C. W. Woods, E. W. Petzold, A. G. Schmidt, I. T. Teng, T. Zhou, P. D. Kwong, J. R. Mascola, B. S. Graham, I. N. Moore, R. Seder, H. Andersen, M. G. Lewis, D. C. Montefiori, G. D. Sempowski, R. S. Baric, P. Acharya, B. F. Haynes, K. O. Saunders, In vitro and in vivo functions of SARS-CoV-2 infection-enhancing and neutralizing antibodies. *Cell* **184**, 4203-4219 e4232 (2021).

50. A. Z. Wec, D. Wrapp, A. S. Herbert, D. P. Maurer, D. Haslwanter, M. Sakharkar, R. K. Jangra, M. E. Dieterle, A. Lilov, D. Huang, L. V. Tse, N. V. Johnson, C. L. Hsieh, N. Wang, J. H. Nett, E. Champney, I. Burnina, M. Brown, S. Lin, M. Sinclair, C. Johnson, S. Pudi, R. Bortz, 3rd, A. S. Wirchnianski, E. Laudermilch, C. Florez, J. M. Fels, C. M. O'Brien, B. S. Graham, D. Nemazee, D. R. Burton, R. S. Baric, J. E. Voss, K. Chandran, J. M. Dye, J. S. McLellan, L. M. Walker, Broad neutralization of SARS-related viruses by human monoclonal antibodies. *Science* **369**, 731-736 (2020).

51. X. Chi, R. Yan, J. Zhang, G. Zhang, Y. Zhang, M. Hao, Z. Zhang, P. Fan, Y. Dong, Y. Yang, Z. Chen, Y. Guo, J. Zhang, Y. Li, X. Song, Y. Chen, L. Xia, L. Fu, L. Hou, J. Xu,

C. Yu, J. Li, Q. Zhou, W. Chen, A neutralizing human antibody binds to the N-terminal domain of the Spike protein of SARS-CoV-2. *Science* **369**, 650-655 (2020).

52. G. Song, W. T. He, S. Callaghan, F. Anzanello, D. Huang, J. Ricketts, J. L. Torres, N. Beutler, L. Peng, S. Vargas, J. Cassell, M. Parren, L. Yang, C. Ignacio, D. M. Smith, J. E. Voss, D. Nemazee, A. B. Ward, T. Rogers, D. R. Burton, R. Andrabi, Cross-reactive serum and memory B-cell responses to spike protein in SARS-CoV-2 and endemic coronavirus infection. *Nat Commun* **12**, 2938 (2021).
53. E. Andreano, E. Nicastri, I. Paciello, P. Pileri, N. Manganaro, G. Piccini, A. Manenti, E. Pantano, A. Kabanova, M. Troisi, F. Vacca, D. Cardamone, C. De Santi, J. L. Torres, G. Ozorowski, L. Benincasa, H. Jang, C. Di Genova, L. Depau, J. Brunetti, C. Agrati, M. R. Capobianchi, C. Castilletti, A. Emiliozzi, M. Fabbiani, F. Montagnani, L. Bracci, G. Sautto, T. M. Ross, E. Montomoli, N. Temperton, A. B. Ward, C. Sala, G. Ippolito, R. Rappuoli, Extremely potent human monoclonal antibodies from COVID-19 convalescent patients. *Cell* **184**, 1821-1835 e1816 (2021).
54. H. Liu, C. I. Kaku, G. Song, M. Yuan, R. Andrabi, D. R. Burton, L. M. Walker, I. A. Wilson, A recurring YYDRxG pattern in broadly neutralizing antibodies to a conserved site on SARS-CoV-2, variants of concern, and related viruses. *bioRxiv*, 2021.2012.2015.472864 (2021).
55. C. Soto, R. G. Bombardi, A. Branchizio, N. Kose, P. Matta, A. M. Sevy, R. S. Sinkovits, P. Gilchuk, J. A. Finn, J. E. Crowe, Jr., High frequency of shared clonotypes in human B cell receptor repertoires. *Nature* **566**, 398-402 (2019).
56. C. Liu, D. Zhou, R. Nutalai, H. M. E. Duyvesteyn, A. Tuekprakhon, H. M. Ginn, W. Dejnirattisai, P. Supasa, A. J. Mentzer, B. Wang, J. B. Case, Y. Zhao, D. T. Skelly, R. E. Chen, S. A. Johnson, T. G. Ritter, C. Mason, T. Malik, N. Temperton, N. G. Paterson, M. A. Williams, D. R. Hall, D. K. Clare, A. Howe, P. J. R. Goulder, E. E. Fry, M. S. Diamond, J. Mongkolsapaya, J. Ren, D. I. Stuart, G. R. Screaton, The antibody response to SARS-CoV-2 Beta underscores the antigenic distance to other variants. *Cell Host Microbe* **30**, 53-68 e12 (2022).
57. S. M. Reincke, M. Yuan, H. C. Kornau, V. M. Corman, S. van Hoof, E. Sanchez-Sendin, M. Ramberger, W. Yu, Y. Hua, H. Tien, M. L. Schmidt, T. Schwarz, L. M. Jeworowski, S. E. Brandl, H. F. Rasmussen, M. A. Homeyer, L. Stoffler, M. Barner, D. Kunkel, S. Huo, J. Horler, N. von Wardenburg, I. Kroidl, T. M. Eser, A. Wieser, C. Geldmacher, M. Hoelscher, H. Ganzer, G. Weiss, D. Schmitz, C. Drosten, H. Pruss, I. A. Wilson, J. Kreye, SARS-CoV-2 Beta variant infection elicits potent lineage-specific and cross-reactive antibodies. *Science* **375**, 782-787 (2022).
58. C. Kreer, M. Zehner, T. Weber, M. S. Ercanoglu, L. Gieselmann, C. Rohde, S. Halwe, M. Korenkov, P. Schommers, K. Vanshylla, V. Di Cristanziano, H. Janicki, R. Brinker, A. Ashurov, V. Krahling, A. Kupke, H. Cohen-Dvashi, M. Koch, J. M. Eckert, S. Lederer, N. Pfeifer, T. Wolf, M. Vehreschild, C. Wendtner, R. Diskin, H. Gruell, S. Becker, F. Klein, Longitudinal Isolation of Potent Near-Germline SARS-CoV-2-Neutralizing Antibodies from COVID-19 Patients. *Cell* **182**, 843-854 e812 (2020).
59. E. Seydoux, L. J. Homad, A. J. MacCamy, K. R. Parks, N. K. Hurlburt, M. F. Jennewein, N. R. Akins, A. B. Stuart, Y. H. Wan, J. Feng, R. E. Whaley, S. Singh, M. Boeckh, K. W. Cohen, M. J. McElrath, J. A. Englund, H. Y. Chu, M. Pancera, A. T. McGuire, L. Stamatatos, Analysis of a SARS-CoV-2-Infected Individual Reveals Development of

Potent Neutralizing Antibodies with Limited Somatic Mutation. *Immunity* **53**, 98-105 e105 (2020).

60. T. F. Rogers, F. Zhao, D. Huang, N. Beutler, A. Burns, W. T. He, O. Limbo, C. Smith, G. Song, J. Woehl, L. Yang, R. K. Abbott, S. Callaghan, E. Garcia, J. Hurtado, M. Parren, L. Peng, S. Ramirez, J. Ricketts, M. J. Ricciardi, S. A. Rawlings, N. C. Wu, M. Yuan, D. M. Smith, D. Nemazee, J. R. Teijaro, J. E. Voss, I. A. Wilson, R. Andrabi, B. Briney, E. Landais, D. Sok, J. G. Jardine, D. R. Burton, Isolation of potent SARS-CoV-2 neutralizing antibodies and protection from disease in a small animal model. *Science* **369**, 956-963 (2020).
61. S. C. A. Nielsen, F. Yang, K. J. L. Jackson, R. A. Hoh, K. Roltgen, G. H. Jean, B. A. Stevens, J. Y. Lee, A. Rustagi, A. J. Rogers, A. E. Powell, M. Hunter, J. Najeeb, A. R. Otrelo-Cardoso, K. E. Yost, B. Daniel, K. C. Nadeau, H. Y. Chang, A. T. Satpathy, T. S. Jardetzky, P. S. Kim, T. T. Wang, B. A. Pinsky, C. A. Blish, S. D. Boyd, Human B Cell Clonal Expansion and Convergent Antibody Responses to SARS-CoV-2. *Cell Host Microbe* **28**, 516-525 e515 (2020).
62. A. K. Wheatley, P. Pymm, R. Esterbauer, M. H. Dietrich, W. S. Lee, D. Drew, H. G. Kelly, L. J. Chan, F. L. Mordant, K. A. Black, A. Adair, H. X. Tan, J. A. Juno, K. M. Wragg, T. Amarasena, E. Lopez, K. J. Selva, E. R. Haycroft, J. P. Cooney, H. Venugopal, L. L. Tan, O. N. MT, C. C. Allison, D. Cromer, M. P. Davenport, R. A. Bowen, A. W. Chung, M. Pellegrini, M. T. Liddament, A. Glukhova, K. Subbarao, S. J. Kent, W. H. Tham, Landscape of human antibody recognition of the SARS-CoV-2 receptor binding domain. *Cell Rep* **37**, 109822 (2021).
63. Y. Zhou, Z. Liu, S. Li, W. Xu, Q. Zhang, I. T. Silva, C. Li, Y. Wu, Q. Jiang, Z. Liu, Q. Wang, Y. Guo, J. Wu, C. Gu, X. Cai, D. Qu, C. T. Mayer, X. Wang, S. Jiang, T. Ying, Z. Yuan, Y. Xie, Y. Wen, L. Lu, Q. Wang, Enhancement versus neutralization by SARS-CoV-2 antibodies from a convalescent donor associates with distinct epitopes on the RBD. *Cell Rep* **34**, 108699 (2021).
64. A. R. Shiakolas, K. J. Kramer, N. V. Johnson, S. C. Wall, N. Suryadevara, D. Wrapp, S. Periasamy, K. A. Pilewski, N. Raju, R. Nargi, R. E. Sutton, L. M. Walker, I. Setliff, J. E. Crowe, Jr., A. Bukreyev, R. H. Carnahan, J. S. McLellan, I. S. Georgiev, Efficient discovery of SARS-CoV-2-neutralizing antibodies via B cell receptor sequencing and ligand blocking. *Nat Biotechnol*, (2022).
65. J. S. Turner, J. A. O'Halloran, E. Kalaidina, W. Kim, A. J. Schmitz, J. Q. Zhou, T. Lei, M. Thapa, R. E. Chen, J. B. Case, F. Amanat, A. M. Rauseo, A. Haile, X. Xie, M. K. Klebert, T. Suessen, W. D. Middleton, P. Y. Shi, F. Krammer, S. A. Teefey, M. S. Diamond, R. M. Presti, A. H. Ellebedy, SARS-CoV-2 mRNA vaccines induce persistent human germinal centre responses. *Nature* **596**, 109-113 (2021).
66. C. Graham, J. Seow, I. Huettner, H. Khan, N. Kouphou, S. Acors, H. Winstone, S. Pickering, R. P. Galao, L. Dupont, M. J. Lista, J. M. Jimenez-Guardeno, A. G. Laing, Y. Wu, M. Joseph, L. Muir, M. J. van Gils, W. M. Ng, H. M. E. Duyvesteyn, Y. Zhao, T. A. Bowden, M. Shankar-Hari, A. Rosa, P. Cherepanov, L. E. McCoy, A. C. Hayday, S. J. D. Neil, M. H. Malim, K. J. Doores, Neutralization potency of monoclonal antibodies recognizing dominant and subdominant epitopes on SARS-CoV-2 Spike is impacted by the B.1.1.7 variant. *Immunity* **54**, 1276-1289 e1276 (2021).
67. L. A. VanBlargan, J. M. Errico, P. J. Halfmann, S. J. Zost, J. E. Crowe, Jr., L. A. Purcell, Y. Kawaoka, D. Corti, D. H. Fremont, M. S. Diamond, An infectious SARS-CoV-2

B.1.1.529 Omicron virus escapes neutralization by therapeutic monoclonal antibodies. *Nat Med*, (2022).

68. K. S. Corbett, M. C. Nason, B. Flach, M. Gagne, S. O'Connell, T. S. Johnston, S. N. Shah, V. V. Edara, K. Floyd, L. Lai, C. McDanal, J. R. Francica, B. Flynn, K. Wu, A. Choi, M. Koch, O. M. Abiona, A. P. Werner, J. I. Moliva, S. F. Andrew, M. M. Donaldson, J. Fintzi, D. R. Flebbe, E. Lamb, A. T. Noe, S. T. Nurmukhambetova, S. J. Provost, A. Cook, A. Dodson, A. Faudree, J. Greenhouse, S. Kar, L. Pessaint, M. Porto, K. Steingrebe, D. Valentin, S. Zouantcha, K. W. Bock, M. Minai, B. M. Nagata, R. van de Wetering, S. Boyoglu-Barnum, K. Leung, W. Shi, E. S. Yang, Y. Zhang, J. M. Todd, L. Wang, G. S. Alvarado, H. Andersen, K. E. Foulds, D. K. Edwards, J. R. Mascola, I. N. Moore, M. G. Lewis, A. Carfi, D. Montefiori, M. S. Suthar, A. McDermott, M. Roederer, N. J. Sullivan, D. C. Douek, B. S. Graham, R. A. Seder, Immune correlates of protection by mRNA-1273 vaccine against SARS-CoV-2 in nonhuman primates. *Science* **373**, eabj0299 (2021).
69. P. B. Gilbert, D. C. Montefiori, A. B. McDermott, Y. Fong, D. Benkeser, W. Deng, H. Zhou, C. R. Houchens, K. Martins, L. Jayashankar, F. Castellino, B. Flach, B. C. Lin, S. O'Connell, C. McDanal, A. Eaton, M. Sarzotti-Kelsoe, Y. Lu, C. Yu, B. Borate, L. W. P. van der Laan, N. S. Hejazi, C. Huynh, J. Miller, H. M. El Sahly, L. R. Baden, M. Baron, L. De La Cruz, C. Gay, S. Kalams, C. F. Kelley, M. P. Andrasik, J. G. Kublin, L. Corey, K. M. Neuzil, L. N. Carpp, R. Pajon, D. Follmann, R. O. Donis, R. A. Koup, Immune correlates analysis of the mRNA-1273 COVID-19 vaccine efficacy clinical trial. *Science* **375**, 43-50 (2022).
70. D. Cromer, M. Steain, A. Reynaldi, T. E. Schlub, A. K. Wheatley, J. A. Juno, S. J. Kent, J. A. Triccas, D. S. Khoury, M. P. Davenport, Neutralising antibody titres as predictors of protection against SARS-CoV-2 variants and the impact of boosting: a meta-analysis. *Lancet Microbe* **3**, e52-e61 (2022).
71. A. J. Greaney, T. N. Starr, R. T. Eguia, A. N. Loes, K. Khan, F. Karim, S. Cele, J. E. Bowen, J. K. Logue, D. Corti, D. Veesler, H. Y. Chu, A. Sigal, J. D. Bloom, A SARS-CoV-2 variant elicits an antibody response with a shifted immunodominance hierarchy. *PLoS Pathog* **18**, e1010248 (2022).
72. S. A. Robinson, M. I. J. Raybould, C. Schneider, W. K. Wong, C. Marks, C. M. Deane, Epitope profiling using computational structural modelling demonstrated on coronavirus-binding antibodies. *PLoS Comput Biol* **17**, e1009675 (2021).
73. K. S. Corbett, A. P. Werner, S. O. Connell, M. Gagne, L. Lai, J. I. Moliva, B. Flynn, A. Choi, M. Koch, K. E. Foulds, S. F. Andrew, D. R. Flebbe, E. Lamb, S. T. Nurmukhambetova, S. J. Provost, K. W. Bock, M. Minai, B. M. Nagata, A. V. Ry, Z. Flinchbaugh, T. S. Johnston, E. B. Mokhtari, P. Mudvari, A. R. Henry, F. Laboune, B. Chang, M. Porto, J. Wear, G. S. Alvarado, S. Boyoglu-Barnum, J. M. Todd, B. Bart, A. Cook, A. Dodson, L. Pessaint, K. Steingrebe, S. Elbashir, M. Sriparna, A. Pekosz, H. Andersen, K. Wu, D. K. Edwards, S. Kar, M. G. Lewis, E. Boritz, I. N. Moore, A. Carfi, M. S. Suthar, A. McDermott, M. Roederer, M. C. Nason, N. J. Sullivan, D. C. Douek, B. S. Graham, R. A. Seder, mRNA-1273 protects against SARS-CoV-2 beta infection in nonhuman primates. *Nat Immunol* **22**, 1306-1315 (2021).
74. M. Gagne, K. S. Corbett, B. J. Flynn, K. E. Foulds, D. A. Wagner, S. F. Andrew, J. M. Todd, C. C. Honeycutt, L. McCormick, S. T. Nurmukhambetova, M. E. Davis-Gardner, L. Pessaint, K. W. Bock, B. M. Nagata, M. Minai, A. P. Werner, J. I. Moliva, C. Tucker, C. G. Lorang, B. Zhao, E. McCarthy, A. Cook, A. Dodson, I. T. Teng, P. Mudvari, J. Roberts-

Torres, F. Laboune, L. Wang, A. Goode, S. Kar, S. Boyoglu-Barnum, E. S. Yang, W. Shi, A. Ploquin, N. Doria-Rose, A. Carfi, J. R. Mascola, E. A. Boritz, D. K. Edwards, H. Andersen, M. G. Lewis, M. S. Suthar, B. S. Graham, M. Roederer, I. N. Moore, M. C. Nason, N. J. Sullivan, D. C. Douek, R. A. Seder, Protection from SARS-CoV-2 Delta one year after mRNA-1273 vaccination in rhesus macaques coincides with anamnestic antibody response in the lung. *Cell* **185**, 113-130 e115 (2022).

75. J. F. Scheid, C. O. Barnes, B. Eraslan, A. Hudak, J. R. Keeffe, L. A. Cosimi, E. M. Brown, F. Muecksch, Y. Weisblum, S. Zhang, T. Delorey, A. E. Woolley, F. Ghantous, S. M. Park, D. Phillips, B. Tusi, K. E. Huey-Tubman, A. A. Cohen, P. N. P. Gnanapragasam, K. Rzasa, T. Hatziioanno, M. A. Durney, X. Gu, T. Tada, N. R. Landau, A. P. West, Jr., O. Rozenblatt-Rosen, M. S. Seaman, L. R. Baden, D. B. Graham, J. Deguine, P. D. Bieniasz, A. Regev, D. Hung, P. J. Bjorkman, R. J. Xavier, B cell genomics behind cross-neutralization of SARS-CoV-2 variants and SARS-CoV. *Cell* **184**, 3205-3221 e3224 (2021).

76. A. Pegu, S. E. O'Connell, S. D. Schmidt, S. O'Dell, C. A. Talana, L. Lai, J. Albert, E. Anderson, H. Bennett, K. S. Corbett, B. Flach, L. Jackson, B. Leav, J. E. Ledgerwood, C. J. Luke, M. Makowski, M. C. Nason, P. C. Roberts, M. Roederer, P. A. Rebolledo, C. A. Rostad, N. G. Rouphael, W. Shi, L. Wang, A. T. Widge, E. S. Yang, R. N. A. S. G. s. s. m, J. H. Beigel, B. S. Graham, J. R. Mascola, M. S. Suthar, A. B. McDermott, N. A. Doria-Rose, J. Arega, J. H. Beigel, W. Buchanan, M. Elsafy, B. Hoang, R. Lampley, A. Kolhekar, H. Koo, C. Luke, M. Makhene, S. Nayak, R. Pikaart-Tautges, P. C. Roberts, J. Russell, E. Sindall, J. Albert, P. Kunwar, M. Makowski, E. J. Anderson, A. Bechnak, M. Bower, A. F. Camacho-Gonzalez, M. Collins, A. Drobeniuc, V. V. Edara, S. Edupuganti, K. Floyd, T. Gibson, C. M. G. Ackerley, B. Johnson, S. Kamidani, C. Kao, C. Kelley, L. Lai, H. Macenczak, M. P. McCullough, E. Peters, V. K. Phadke, P. A. Rebolledo, C. A. Rostad, N. Rouphael, E. Scherer, A. Sherman, K. Stephens, M. S. Suthar, M. Teherani, J. Traenkner, J. Winston, I. Yildirim, L. Barr, J. Benoit, B. Carste, J. Choe, M. Dunstan, R. Erolin, J. Ffitch, C. Fields, L. A. Jackson, E. Kiniry, S. Lasicka, S. Lee, M. Nguyen, S. Pimienta, J. Suyehira, M. Witte, H. Bennett, N. E. Altaras, A. Carfi, M. Hurley, B. Leav, R. Pajon, W. Sun, T. Zaks, R. N. Coler, S. E. Larsen, K. M. Neuzil, L. C. Lindesmith, D. R. Martinez, J. Munt, M. Mallory, C. Edwards, R. S. Baric, N. M. Berkowitz, E. A. Boritz, K. Carlton, K. S. Corbett, P. Costner, A. Creanga, N. A. Doria-Rose, D. C. Douek, B. Flach, M. Gaudinski, I. Gordon, B. S. Graham, L. Holman, J. E. Ledgerwood, K. Leung, B. C. Lin, M. K. Louder, J. R. Mascola, A. B. McDermott, K. M. Morabito, L. Novik, S. O'Connell, S. O'Dell, M. Padilla, A. Pegu, S. D. Schmidt, W. Shi, P. A. Swanson, 2nd, C. A. Talana, L. Wang, A. T. Widge, E. S. Yang, Y. Zhang, J. D. Chappell, M. R. Denison, T. Hughes, X. Lu, A. J. Pruijssers, L. J. Stevens, C. M. Posavad, M. Gale, Jr., V. Menachery, P. Y. Shi, Durability of mRNA-1273 vaccine-induced antibodies against SARS-CoV-2 variants. *Science* **373**, 1372-1377 (2021).

77. T. Zhou, I. T. Teng, A. S. Olia, G. Cerutti, J. Gorman, A. Nazzari, W. Shi, Y. Tsybovsky, L. Wang, S. Wang, B. Zhang, Y. Zhang, P. S. Katsamba, Y. Petrova, B. B. Banach, A. S. Fahad, L. Liu, S. N. Lopez Acevedo, B. Madan, M. Oliveira de Souza, X. Pan, P. Wang, J. R. Wolfe, M. Yin, D. D. Ho, E. Phung, A. DiPiazza, L. A. Chang, O. M. Abiona, K. S. Corbett, B. J. DeKosky, B. S. Graham, J. R. Mascola, J. Misasi, T. Ruckwardt, N. J. Sullivan, L. Shapiro, P. D. Kwong, Structure-Based Design with Tag-Based Purification

and In-Process Biotinylation Enable Streamlined Development of SARS-CoV-2 Spike Molecular Probes. *Cell Rep* **33**, 108322 (2020).

78. I. T. Teng, A. F. Nazzari, M. Choe, T. Liu, M. O. de Souza, Y. Petrova, Y. Tsybovsky, S. Wang, B. Zhang, M. Artamonov, B. Madan, A. Huang, S. N. Lopez Acevedo, X. Pan, T. J. Ruckwardt, B. J. DeKosky, J. R. Mascola, J. Misasi, N. J. Sullivan, T. Zhou, P. D. Kwong, Molecular probes of spike ectodomain and its subdomains for SARS-CoV-2 variants, Alpha through Omicron. *bioRxiv*, (2021).
79. S. J. Krebs, Y. D. Kwon, C. A. Schramm, W. H. Law, G. Donofrio, K. H. Zhou, S. Gift, V. Dussupt, I. S. Georgiev, S. Schatzle, J. R. McDaniel, Y. T. Lai, M. Sastry, B. Zhang, M. C. Jarosinski, A. Ransier, A. L. Chenine, M. Asokan, R. T. Bailer, M. Bose, A. Cagigi, E. M. Cale, G. Y. Chuang, S. Darko, J. I. Driscoll, A. Druz, J. Gorman, F. Laboune, M. K. Louder, K. McKee, L. Mendez, M. A. Moody, A. M. O'Sullivan, C. Owen, D. Peng, R. Rawi, E. Sanders-Buell, C. H. Shen, A. R. Shiakolas, T. Stephens, Y. Tsybovsky, C. Tucker, R. Verardi, K. Wang, J. Zhou, T. Zhou, G. Georgiou, S. M. Alam, B. F. Haynes, M. Rolland, G. R. Matyas, V. R. Polonis, A. B. McDermott, D. C. Douek, L. Shapiro, S. Tovanabutra, N. L. Michael, J. R. Mascola, M. L. Robb, P. D. Kwong, N. A. Doria-Rose, Longitudinal Analysis Reveals Early Development of Three MPER-Directed Neutralizing Antibody Lineages from an HIV-1-Infected Individual. *Immunity* **50**, 677-691 e613 (2019).
80. A. A. Upadhyay, R. C. Kauffman, A. N. Wolabaugh, A. Cho, N. B. Patel, S. M. Reiss, C. Havenar-Daughton, R. A. Dawoud, G. K. Tharp, I. Sanz, B. Pulendran, S. Crotty, F. E. Lee, J. Wrammert, S. E. Bosinger, BALDR: a computational pipeline for paired heavy and light chain immunoglobulin reconstruction in single-cell RNA-seq data. *Genome Med* **10**, 20 (2018).
81. C. A. Schramm, Z. Sheng, Z. Zhang, J. R. Mascola, P. D. Kwong, L. Shapiro, SONAR: A High-Throughput Pipeline for Inferring Antibody Ontogenies from Longitudinal Sequencing of B Cell Transcripts. *Front Immunol* **7**, 372 (2016).
82. Y. Hao, S. Hao, E. Andersen-Nissen, W. M. Mauck, 3rd, S. Zheng, A. Butler, M. J. Lee, A. J. Wilk, C. Darby, M. Zager, P. Hoffman, M. Stoeckius, E. Papalexi, E. P. Mimitou, J. Jain, A. Srivastava, T. Stuart, L. M. Fleming, B. Yeung, A. J. Rogers, J. M. McElrath, C. A. Blish, R. Gottardo, P. Smibert, R. Satija, Integrated analysis of multimodal single-cell data. *Cell* **184**, 3573-3587 e3529 (2021).
83. T. Rognes, T. Flouri, B. Nichols, C. Quince, F. Mahe, VSEARCH: a versatile open source tool for metagenomics. *PeerJ* **4**, e2584 (2016).

Acknowledgements

The authors would like to thank the members of the VRC 200 Study Team for their role in collecting samples that were used in this study: Lesia Drupolic, Lasonji Holman, Maria Burgos Florez, Charla Andrews, Britta Flach, Emily Coates, Obrimpong Amoa-Awua, Jennifer Cunningham, Pamela Costner, Floreliz Mendoza, William Whalen, Jamie Saunders, Laura Novik, Aba Eshun, Anita Arthur, Xiaolin Wang, Karen Parker, Abidemi Ola, Catina Evans, Jennifer Phipps, Pernell Williams, Justine Jones, Jackie Stephens, Jumoke Gbadebo, Preeti Apete, Renunda Hicks, LaShawn Requillman, Alison Beck, Seemal Awan, Richard Wu, Priya Kamath, Olga Trofymenko, Sarah Plummer, Nina Berkowitz, Olga Vasilenko, and Iris Pittman.

The authors also thank Dr. Steven De Rosa (Fred Hutchinson Cancer Center) for providing a 28-color flow cytometry panel which we modified for our study and David Ambrozak for assistance with cell sorting.

Funding

This work was funded in part by the Intramural Research Program of the Vaccine Research Center, National Institute of Allergy and Infection Disease, National Institutes of Health.

Author Contributions

Conceptualization: NSL, CAS, DCD

Data curation: MM, CAS

Formal Analysis: NSL, MM, TSJ, DAW, LW, KB, SRN, SOC, KLB, CAS

Investigation: NSL, MM, TSJ, DAW, ARH, LW, KB, WPB, SDS, DM, CGL, BZ, KLB, JRT, RLD, LP, JW, CAT

Methodology: TSJ, DCD

Resources: ESY, YZ, SOD, MC, AS, KL, WS, RK, AB, TZ, JR, SV, AA, LN, AW, IG, M Guech, ITT, EP, TJR

Supervision: AP, JM, NADR, M Guadinski, RAK, PDK, ABM, SA, TWS, IL, JRM, NJS, CAS, DCD

Visualization: NSL, MM, TSJ, DAW, KLB, CAS, DCD

Writing – original draft: NSL, MM, TSJ, CAS, DCD

Writing – review & editing: all authors

Competing interests

None declared.

Data and materials availability

All data and materials are available upon request.

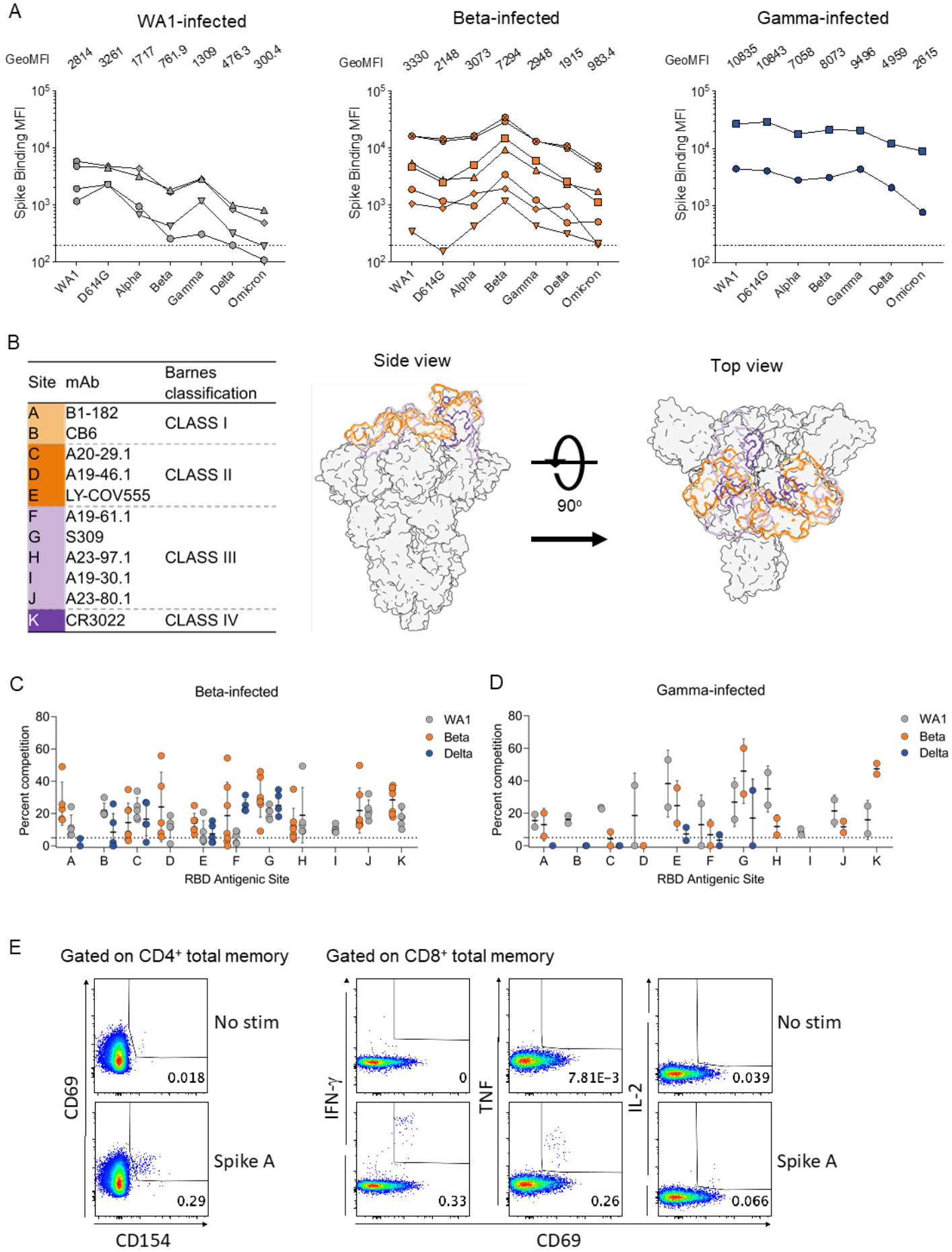

Supplemental Figure 1: Additional serology and epitope mapping data. **A)** Antibody binding titers against multiple variants assessed by cell surface binding assay; **B)** Structural schematic of spike protein showing epitopes from monoclonal antibodies used for RBD epitope mapping by competition assay; **C)** Epitope mapping of Beta-infected individuals on WA1, Beta and Delta spike proteins; **D)** Epitope mapping of Gamma-infected individuals on WA1, Beta and Delta spike proteins; **E)** Gating strategy for T cell response analysis.

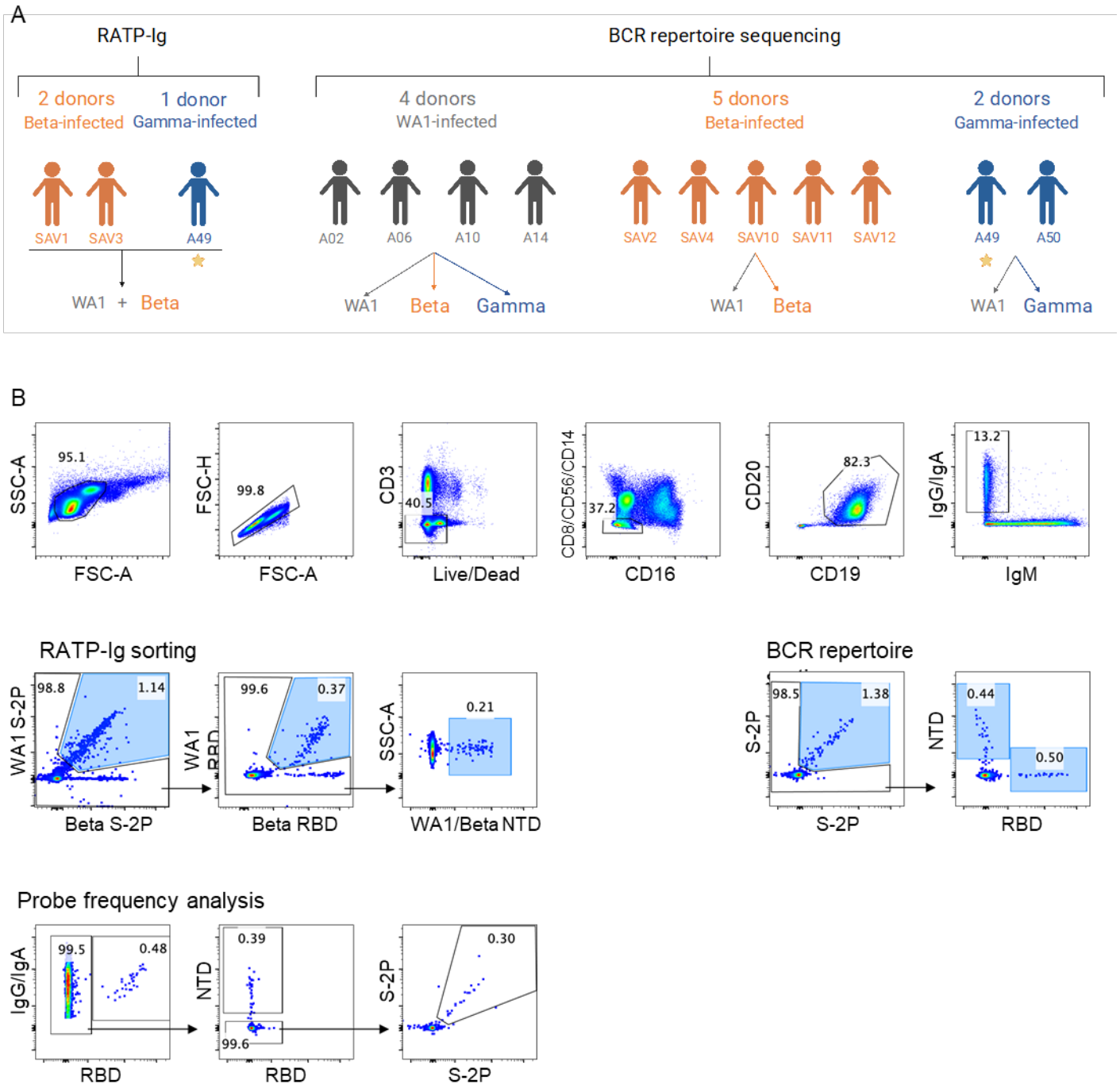

Supplemental Figure 2: Antigen-specific B cell sorting. (**A**) Arrows indicate probes used for sorting antigen-specific B cells from each group of convalescent individuals. The individual marked with a star was used for both RATP-Ig and total BCR repertoire sequencing. (**B**) Flow cytometry representative plots and gating strategies for B cell sorting and analysis; final sort gates are shown in blue.

1239

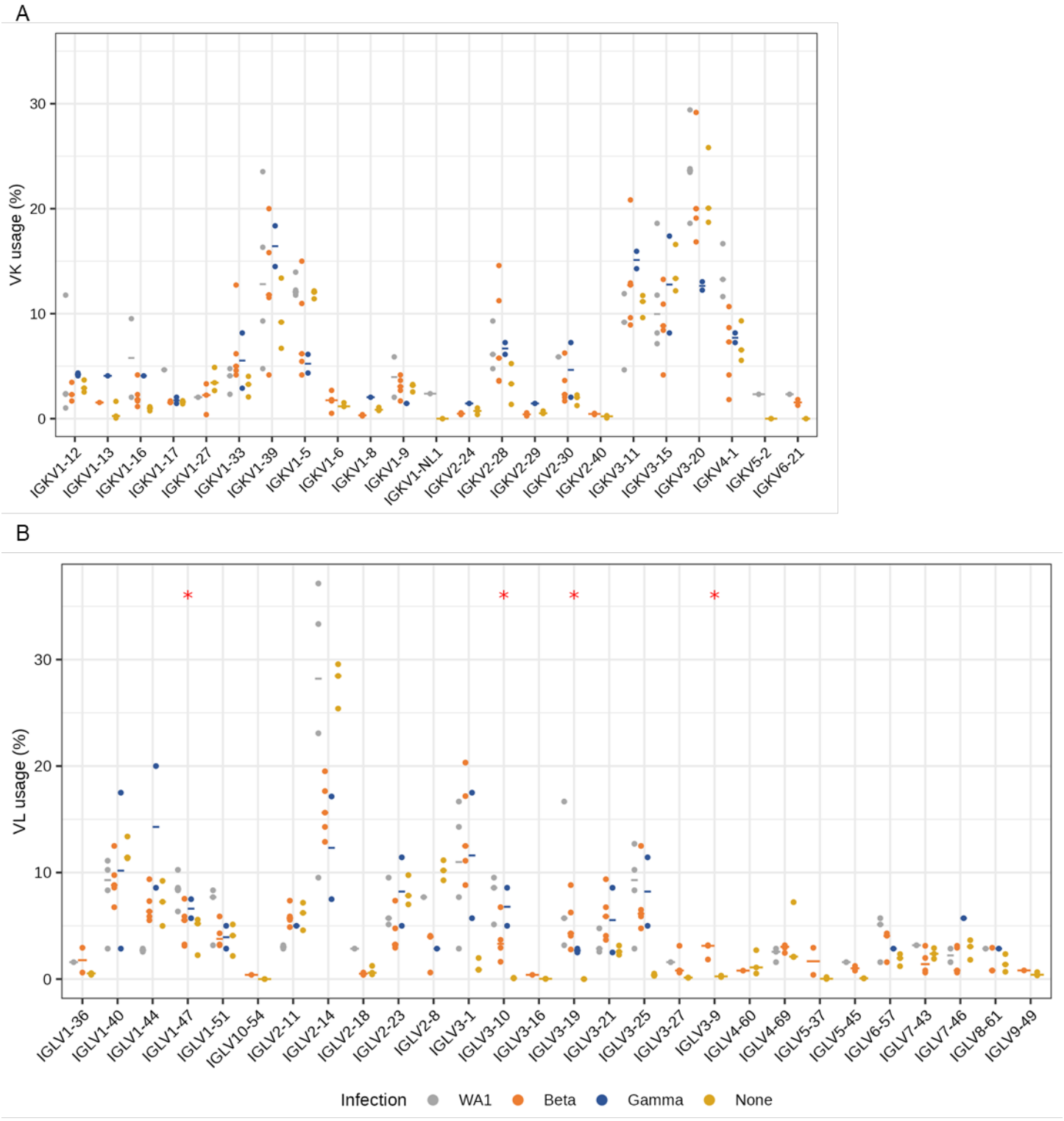

Supplementary Figure 3: SARS-CoV-2-specific light chain V gene usage frequencies. (A) Kappa and (B) Lambda chain V gene repertoire analysis by infecting variant, with WA1, Beta and Gamma shown in grey, orange and blue, respectively, and data from pre-pandemic controls in yellow. The x-axis shows all germline genes used; the y-axis represents the percent of individual gene usage. Stars indicate genes with at least one significant difference between groups; pairwise comparisons using the Dunn test are in Table S4.

	Infecting virus	Days after symptoms	Disease severity	Date of collection	Gender	Age
A02	WA1	28	Mild	Mar-20	Male	39
A06	WA1	34	Mild	Apr-20	Female	59
A10	WA1	33	Moderate	Apr-20	Female	67
A14	WA1	34	Mild	Apr-20	Male	27
SAV1	Beta	33	Severe	Jan-21	Male	60
SAV2	Beta	33	Mild	Jan-21	Male	35
SAV3	Beta	30	Mild	Jan-21	Female	58
SAV4	Beta	28	Mild	Jan-21	Female	30
SAV10	Beta	38	Mild	Feb-21	Female	43
SAV11	Beta	37	Mild	Feb-21	Female	52
SAV12	Beta	35	Mild	Feb-21	Male	44
A49	Gamma	24	Moderate	Jan-21	Female	53
A50	Gamma	17	Mild	Jan-21	Male	32

Supplementary Table 1: Details of the study cohort.

Sample ID	Infected with:	Spike variant		
		WA1	Beta	Delta
A02	WA1		below LLOQ	below LLOQ
A06	WA1		below LLOQ	below LLOQ
A10	WA1		below LLOQ	below LLOQ
A14	WA1		below LLOQ	
SAV1	Beta			
SAV2	Beta	below LLOQ		below LLOQ
SAV3	Beta			
SAV4	Beta			
SAV10	Beta	below LLOQ		below LLOQ
SAV11	Beta			
SAV12	Beta			
A49	Gamma			
A50	Gamma			

1244

1245 **Supplementary Table 2:** Serum epitope competition

1246

		SARS-CoV-2 Probe:						Total paired sequences by subject:
		WA1		Beta		Gamma		
WA1-infected	A02	3/23	(13%)	3/8	(28%)	4/13	(31%)	10
	A06	11/140	(8%)	4/74	(5%)	9/62	(15%)	24
	A10	9/87	(10%)	10/46	(22%)	11/34	(32%)	30
	A14	20/205	(10%)	14/76	(18%)	23/79	(29%)	57
Beta-Infected	SAV2	2/104	(2%)	14/214	(7%)	N/A		16
	SAV4	16/328	(5%)	40/630	(6%)	N/A		56
	SAV10	6/102	(6%)	12/131	(9%)	N/A		18
	SAV11	39/645	(6%)	125/2028	(6%)	N/A		164
	SAV12	32/306	(10%)	97/1318	(7%)	N/A		129
Gamma-Infected	A49	10/129	(8%)	N/A		23/148	(16%)	33
	A50	14/89	(16%)	N/A		37/128	(29%)	51
Total paired sequences by probe:		162		319		107		

Supplementary Table 6: Sample recovery from 10x Genomics-based single cell isolation and sequencing.

Gene	Enriched Group	Median usage frequency, enriched	Depleted Group	Median usage frequency, depleted	Adjusted *P*-value
IGHV1-46	Beta-infected	4.1%	Gamma-infected	1.7%	0.037
IGHV1-46	Beta-infected	4.1%	Control	2.0%	0.045
IGHV1-46	WA1-infected	7.1%	Gamma-infected	1.7%	0.025
IGHV1-46	WA1-infected	7.1%	Control	2.0%	0.041
IGHV3-30	Gamma-infected	29%	Control	7.1%	0.021
IGHV3-30	WA1-infected	18%	Control	7.1%	0.026
IGHV3-49	WA1-infected	6.0%	Control	0.13%	0.021
IGHV4-38-2	WA1-infected	3.1%	Control	0.00%	0.020
IGHV5-51	Beta-infected	4.8%	Control	0.57%	0.021
IGHV5-51	WA1-infected	6.2%	Control	0.57%	0.046
IGLV1-47	WA1-infected	8.5%	Control	5.2%	0.027
IGLV1-47	WA1-infected	8.5%	Beta-infected	5.5%	0.041
IGLV3-9	Beta-infected	3.1%	Control	0.25%	0.050
IGLV3-10	WA1-infected	8.6%	Control	0.07%	0.016
IGLV3-19	Beta-infected	4.3%	Control	0.00%	0.021
IGLV3-19	WA1-infected	5.7%	Control	0.00%	0.036

1251
1252 **Supplementary Table 7:** Significant differences in gene-usage. For genes with a significant difference
1253 detected by the Kruskal-Wallis test (Figs. 4B and S5), the Dunn test was used to find significant pairwise
1254 difference. P values were adjusted for multiple testing using the Benjami-Hochberg procedure.
1255